J. Fluid Mech. (1993), *vol.* 247, *pp.* 79–110

The wake from a cylinder subjected to amplitude-modulated excitation

By M. NAKANO† AND D. ROCKWELL

Department of Mechanical Engineering and Mechanics, 354 Packard Laboratory #19, Lehigh University, Bethlehem, PA 18015, USA

(Received 26 June 1991 and in revised form 15 July 1992)

Controlled, amplitude-modulated excitation of a cylinder at low Reynolds number ($Re = 136$) in the cross-stream direction generates several states of response of the near wake including: a locked-in wake structure, which is periodic at the modulation frequency; a period-doubled wake structure, which is periodic at a frequency half the modulation frequency; and a destabilized structure of the wake, which is periodic at the modulation frequency, but involves substantial phase modulations of the vortex formation relative to the cylinder displacement. The occurrence of each of these states depends upon the dimensionless modulation frequency, as well as the nominal frequency and amplitude of excitation. Transition through states of increasing disorder can be attained by either decreasing the modulation frequency or increasing the amplitude of excitation at a constant value of nominal frequency. These states of response in the near wake are crucial in determining whether the far wake is highly organized or incoherent. Both of these extremes are attainable by proper selection of the parameters of excitation.

1. Introduction

The unsteady structure of the wake from an oscillating bluff body, or cylinder, is important in a variety of applications. The traditional interest in this class of flows has focused on the relationship of the near-wake structure to the unsteady loading on the cylinder. When more than one cylinder is present, such as cylinders in tandem or array configurations, the wakes from the upstream cylinders impinge upon, or buffet, the downstream cylinders. Such configurations include multiple-cable transmission lines, tubes in the leading rows of heat exchanger tube banks, adjacent tall buildings, and neighbouring risers of offshore platforms. In all of these cases, the manner in which the upstream cylinder oscillates, often in a modulated form, strongly influences its wake and therefore the flow structure incident upon a downstream cylinder. In addition to this buffeting type of structural loading, there are other important considerations in engineering practice. They evolve enhancement of mixing and thermal diffusion processes in the near wake, as well as convective heat transfer from the surface of the cylinder. In applications of this sort, manipulation of the near-wake structure is central to enhancement of these processes.

To date, all investigations of forced wakes of bluff bodies have employed purely sinusoidal excitation. Yet, the self-excited oscillation of a bluff body often does not exhibit a sinusoidal form. In some applications, the time-dependent displacement of the body undergoes a relatively strong amplitude modulation, a prime example being the modulated vibration of long towing cables in the field of ocean engineering. The

† On leave from Faculty of Engineering, Yamagata University, Japan.

issue arises as to how such amplitude modulation influences the structure of the downstream wake, including its possible destabilization. This modification of the wake structure would, in turn, have important consequences for the buffeting of downstream bodies. In other types of applications, where it is desired to optimize, for example, the near-wake mixing, amplitude-modulated excitation, with its potential for rapidly altering the degree of coherence of the near-wake structure, may provide an effective means of accomplishing these objectives. The emphasis of this investigation is on the response of the bluff-body wake to amplitude-modulated excitation, with a focus on the manner in which the instantaneous, visualized structure of the wake is related to alterations of its spectral content.

In the absence of extraneous excitation, the near wake of a bluff body can exhibit a region of absolute instability, which provides a self-sustained feedback loop. As a result, there arise highly organized limit-cycle oscillations of the near wake. The interpretation of the near-wake stability mechanism in terms of an absolute instability has been advanced in the series of theoretical studies by Koch (1985), Triantafyllou, Triantafyllou & Chryssostomodis (1986), Monkewitz & Nguyen (1987), and Monkewitz (1988). Since the region of absolute instability must extend over a minimal distance in the streamwise direction in order to generate globally coherent wake oscillations, the term global instability most appropriately describes these flows, as defined by Chomaz, Huerre & Reddekop (1988). Huerre & Monkewitz (1990) provide an overview of the characteristics of globally unstable flows and describe basic techniques for their control and excitation. A major consequence of the globally unstable flow is to give rise to self-excited, limit-cycle oscillations of the near-wake structure; it is well known that these oscillations are relatively insensitive to imposed perturbations, such as small-amplitude displacements of the body. On the other hand, amplitude- or frequency-modulated excitation may provide the potential for breaking the phase-coherent feedback loop in the near-wake region, and thereby have a profound effect on the evolution of the vortex street. This concept has already been suggested in the preliminary studies of Nakano & Rockwell (1991*a*, *b*). It may indeed be possible to manipulate the large-scale vortex formation in ways that are unattainable with purely sinusoidal excitation, which has been addressed in recent years by Griffin & Votaw (1972), Griffin & Ramberg (1974, 1976), Ongoren & Rockwell (1988*a*, *b*), Williamson & Roshko (1988), Rockwell (1990), and works cited therein. Similarly, modulations of the flow past a stationary cylinder may yield substantially different vortical structures, relative to those generated by sinusoidal excitation, as addressed by Couder & Basdevant (1986) and Detemple-Laake & Eckelmann (1989). In turn, such modulated structures in the wake will be related to the forces on the cylinder; Triantafyllou & Karniadakis (1989) have considered the effect of amplitude-modulated excitation on the inclined forces.

The near-wake response of bluff bodies has been interpreted within the framework of chaos in a number of experimental investigations, including those of Sreenivasan (1985), Van Atta & Gharib (1987), Olinger & Sreenivasan (1988) and Karniadakis & Triantafyllou (1989*a*, *b*). The occurrence of chaos in a closed fluid system can provide clues to the anticipated response of the globally unstable wake system, which contains a closed feedback loop in the near-wake region. The classic example of a closed system is the Rayleigh–Bénard instability, which is driven by a temperature difference across the horizontal layer of fluid. Gollub & Benson (1980) reveal a rich variety of routes to turbulence that can be generated within this system. The principal features of these possible routes include: period-doubled (subharmonic) bifurcations; quasi-periodicity and phase-locking; and, among others, intermittent

noise. The corresponding forced excitation of a globally unstable, open flow system of the near wake of a cylinder may exhibit analogous types of response, depending upon the nature of the forcing. Rockwell, Nuzzi & Magness (1991) and Nuzzi, Magness & Rockwell (1992) have observed two successive, period-doubled states of response of the wake from a mildly non-uniform cylinder subjected to sinusoidal excitation. Moreover, the occurrence of a well-defined period doubling in an autonomous mechanical system represented by flow through the end of an elastic cantilevered-mounted pipe, has been characterized by Paidoussis & Moon (1988). Their study provides further encouragement to search for an analogous period doubling in the externally forced response of other types of open flow systems. A particularly interesting issue is the possible generation of new routes to chaos with amplitude-modulated excitation. For instance, there are two principal frequencies associated with the process of amplitude modulation: the primary excitation frequency; and the modulation frequency. The possibility of driving the system to low-order chaotic behaviour through a period-doubled process at the modulation frequency is an intriguing prospect. The manner in which the wake structure passes through states of increasing disorder, owing to changes in the modulation frequency and the amplitude of excitation, is of fundamental interest.

A fascinating issue related to the aforementioned features of the near-wake response can be illustrated with the use of the classical 'lock-in' response diagram of figure 1 representing purely sinusoidal excitation. The region of lock-in, shown on the plane of amplitude versus frequency of excitation, is also known as an Arnol'd tongue. Such lock-in regions or Arnol'd tongues are well known and have been generated in the experimental studies of Olinger & Sreenivasan (1988) and Karniadakis & Triantafyllou (1989*a*), among others. If one first considers a frequency ratio corresponding to matched excitation, i.e. $f_e/f_0^* = 1$, corresponding to forcing at the inherent frequency of vortex formation from the corresponding stationary cylinder, and if the amplitude goes from its maximum value of Y_e to zero during the modulation cycle, then, in a quasi-steady sense, the near-wake vortex formation passes through regions of locked-in and non-locked-in response. An important question is the degree to which this quasi-steady representation is valid. Such a quasi-steady interpretation suggests, for example, that it is not possible to attain locked-in vortex formation during the entire modulation cycle. Of course, the ratio of the excitation frequency f_e to the modulation frequency f_m cannot be represented on this response diagram representing purely sinusoidal excitation; one expects this ratio to be important in determining the existence of a quasi-steady response. Another issue is the effect of the nominal excitation frequency f_e/f_0^*. If it has a value lower than $f_e/f_0^* = 1$, as illustrated in figure 1, then quasi-steady considerations suggest that non-locked-in vortex formation exists over a greater share of the modulation cycle. In this non-locked-in region, one expects the vortex shedding frequency to differ from its locked-in value. Despite the simplicity of this quasi-steady representation, it does imply that a locked-in response may be more difficult to attain for $f_e/f_0^* < 1$ or > 1 than for the case of excitation at $f_e/f_0^* = 1$. Clearly, there are many issues to be pursued if the wake response deviates from the simplified, quasi-steady representation of figure 1. The prospect for attaining rapid destabilization, involving loss of phase coherence of the near-wake oscillation by means of amplitude-modulated excitation, is a fascinating prospect.

All of the foregoing considerations have focused on the near-wake structure. If it is indeed possible to disrupt a highly coherent, self-excited wake instability due to the globally unstable flow in the near-wake region, then one expects this disruption

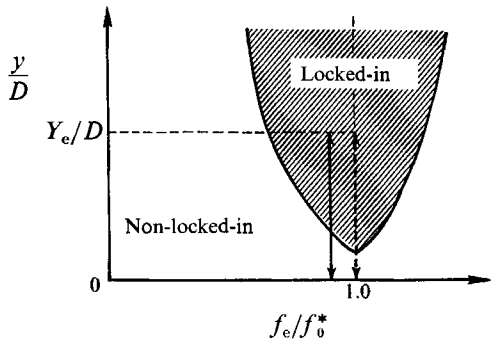

FIGURE 1. Schematic illustrating excursions of cylinder displacement for amplitude-modulated excitation at frequencies corresponding to states of matched excitation ($f_e/f_0^* = 1$) and slightly detuned excitation ($f_e/f_0^* < 1$).

to persist well downstream into the intermediate and far-wake regions. The interesting issue associated with amplitude-modulated excitation is the existence of sideband components above and below the nominal excitation frequency. These sideband components may have relatively low values of frequency, in comparison with the natural frequency of vortex formation. Such low-frequency, long-wavelength perturbations may survive well downstream into the intermediate and far-wake regions, providing disruption of the wake structure beyond that attainable with purely sinusoidal excitation.

2. Experimental system

Experiments were executed in a free-surface water channel, in order to allow accessibility, as well as to isolate the forcing system from the flow. The channel had a cross-section of 610 mm by 610 mm. The brass cylinder of diameter $D = 4.76$ mm had a length to diameter ratio of 109. The Reynolds number based on free-stream velocity and cylinder diameter was $Re = 136$. The inherent vortex formation frequency from the stationary cylinder was $f_0^* = 1.367$ Hz. The cylinder was forced by a computer-controlled Compumotor connected to a traverse table system, located above the free surface. Arbitrary forms of the amplitude-modulated forcing function were programmed into the laboratory microcomputer, which drove the Compumotor system.

Flow visualization involved the hydrogen bubble technique. A 0.025 mm diameter wire was oriented orthogonal to the axis of the cylinder and located a distance of approximately two diameters upstream of the cylinder. This particular wire arrangement was effective for visualizing the near-wake structure. In order to characterize the streamwise variation of the wake structure, successive wire locations at $x/D = 5$, 20 and 35 were employed; the location $x = 0$ corresponds to the centre of the cylinder. The images were recorded on a video system operating at 120 frames per second. The image was transmitted through the bottom of the water channel test section, reflected against a mirror inclined at 45°, then into the video camera. Still photos were taken from the video monitor with a 35 mm camera.

The velocity fields of the near and far wakes were acquired with a 2 W, argon-ion LDA system, operating in the backscatter mode. The output from the counter processor was interfaced with the laboratory microcomputer allowing determination of the spectra of the velocity fluctuations. Analogue filtering was employed to prevent aliasing. The most representative locations for acquiring and interpreting

the velocity spectra of the near- and far-wake response were found to be: $x/D = 5$ and $y/D = Y_e/D + 1.8$, representing the near wake and $x/D = 40$, $y/D = 3$, representing the far wake. The origin of coordinates x and y is at the centre of the cylinder; Y_e is the amplitude of oscillation of the cylinder and D is its diameter. Selection of these locations allowed characterization of the dominant components in the spectra associated with passage of the large-scale structures and their amalgamations due to vortex–vortex interaction.

3. Overview of near-wake response

The cylinder was subjected to amplitude-modulated excitation of the form

$$y(t) = -\tfrac{1}{2}Y_e[1 - \cos(2\pi f_m t)]\sin 2\pi f_e t,$$

in which f_m is the modulation frequency and f_e is the nominal excitation (carrier) frequency. The maximum displacement Y_e of the cylinder is measured from its equilibrium position. Consideration of a range of f_m/f_e and Y_e/D reveals a number of deterministic patterns of vortical structures, which can be classified into basic categories, as shown in figure 2. In defining these categories, we consider the degree to which the vortex patterns are locked-in from one f_e cycle to the next, as well as the periodicity of the flow structure at frequency f_m. In order to illustrate the physics of the wake response, the instantaneous positions of vortices, relative to the instantaneous displacement of the cylinder, are defined below for the domain $0 \leqslant x/D \leqslant 4$, corresponding to the first appearance of fully formed vortical structures.

3.1. f_m *periodic* (*with* f_e *lock-in*)

The basic response of the near-wake vortex street corresponds to the case where the vortices are formed at essentially the same instantaneous displacement from one f_e cycle to the next and the pattern of vortices repeats with each f_m cycle. Figure 2(*a*) shows the timing of formation of the clockwise (dashed line) and counterclockwise (solid line) vortices with respect to the cylinder displacement. In evaluating this timing, photos were taken at instants corresponding to the maximum positive displacement of the cylinder; these instants are represented by the small, solid dots. It is evident that the vortex formation is locked-in from one f_e cycle to the next, that is, the vortices are formed at approximately the same phase of the cylinder displacement. Moreover, this pattern of vortex formation is periodic at frequency f_m, evident by plotting successive f_m cycles beyond that shown in figure 2(*a*). The same type of response can be attained at higher values of the dimensionless modulation frequency f_m/f_e, as illustrated in figure 2(*b*).

3.2. $2f_m$ *periodic* (*non-*f_e *lock-in*)

The period-doubled version of the f_m periodic, f_e lock-in pattern of vortex formation is represented by figure 2(*c*). This pattern does not exhibit lock-in during each f_e cycle for the first f_m cycle, i.e. for the first half of the $2f_m$ cycle. That is, vortices of clockwise and counterclockwise sense are not formed at the same relative positions during successive f_e cycles; in fact, their order of appearance becomes inverted during the first f_m cycle. However, during the second half of the $2f_m$ cycle, there is lock-in during each f_e cycle. This period-doubled ($2f_m$) response therefore represents an increasing state of disorder beyond the f_m periodic, f_e lock-in response defined under the previous category (§3.1). It is, however, more ordered (less chaotic) than the f_m periodic, non-f_e lock-in states defined in §§3.3 and 3.4 for which the vortex pattern is not locked-in over a substantial portion of each f_m cycle.

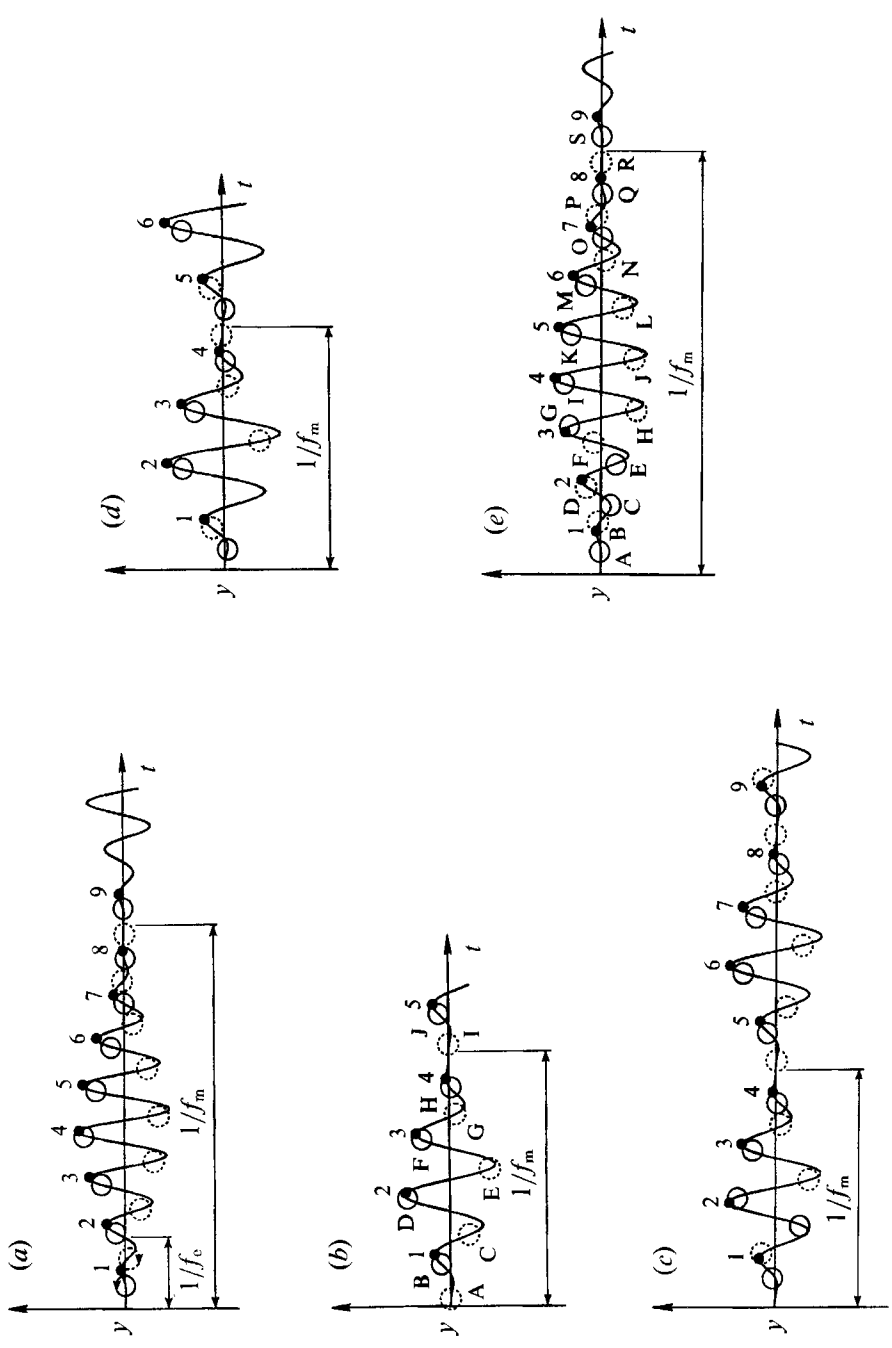

FIGURE 2. Schematics illustrating timing of initially formed clockwise vortices (dashed-line circles) and counterclockwise vortices (solid-line circles) with respect to instantaneous cylinder displacement. Maximum positive displacement of cylinder is indicated by small solid dots.

3.3. f_m *periodic (with non-*f_e *lock-in) – mode* n

It is possible to generate a near-wake structure that is periodic at frequency f_m but not locked-in within each f_e cycle. As illustrated in figure 2(*d*), the first counterclockwise (solid line) vortex is formed at the minimum cylinder displacement, while its successors are formed just prior to the maximum positive displacement. The inverse scenario holds for the clockwise (dashed line) vortices. This non-f_e lock-in response is associated with the lack of formation of a clockwise vortex during the f_e cycle between peak amplitudes 1 and 2.

Irrespective of the particular pattern of vortex formation relative to the cylinder displacement, this category of response involves the formation of n pairs of vortices during each f_m cycle, with n determined by the ratio of the excitation frequency f_e to the modulation frequency f_m, i.e. $n = f_e/f_m$. For the example shown in figure 2(*d*), $f_e/f_m = 4$, there are four pairs of vortices during the period $1/f_m$.

3.4. f_m *periodic (with non-*f_e *lock-in) – mode* $n+1$

Another type of f_m periodic oscillation can arise in the presence of non-locked-in vortex formation within each f_e cycle. It involves the sort of pattern illustrated in figure 2(*e*). During the initial portion of the f_m cycle, the counterclockwise (solid line) vortices represented by A, C, and E are formed near the minimum amplitude of the cylinder displacement, while their successors, G, I, ..., are formed near or at the maximum positive displacement. The converse holds for the clockwise (dashed-line) vortices. This particular modulation results in the formation of an extra pair of vortices during each f_m cycle. The total number of vortex pairs is defined by the relationship $n+1 = f_e/f_m + 1$.

The important consequence of these various types of vortex patterns in the near wake is that they influence not only the spectral content of the velocity field in the near-wake region, giving rise to spectral peaks and various types of spectral broadening there, but also the flow structure and the spectral content in regions of the wake well downstream of the cylinder.

3.5. *Overview of regimes of response*

In the event that the nominal excitation frequency f_e is matched to the inherent instability frequency f_0^* from the stationary cylinder, i.e. $f_e/f_0^* = 1$, then the response of the wake is f_m periodic with f_e lock-in over the entire range of dimensionless modulation frequency f_m/f_e and amplitude Y_e/D. However, when the wake system is slightly detuned from matched excitation at $f_e/f_0^* = 1$, then the regimes described in the foregoing can occur. To illustrate the response of the wake for this detuned condition, an excitation frequency $f_e/f_0^* = 0.95$ is selected. The regimes of response are defined in figure 3. Lock-in at f_e is attainable at relatively low values of Y_e/D and high values of f_m/f_e. For all other domains in figure 3, a locked-in wake structure at f_e is not attainable. The exception is the $2f_m$ periodic state, which exhibits lock-in at f_e during every other f_m cycle. To the right, as well as below this state, there is an f_m periodic response for which non-lock-in at f_e occurs during every f_m cycle. It is possible to drive the wake from its most stable response (f_m periodic, f_e lock-in) to its most unstable response (f_m periodic, non-f_e lock-in) by variation of the amplitude Y_e/D or modulation frequency f_m/f_e. In the present investigation, we address the principal features of these regimes of response in terms of the wake structure and velocity spectra.

Figure 4 shows the effect of nominal excitation frequency f_e/f_0^* on the regimes of

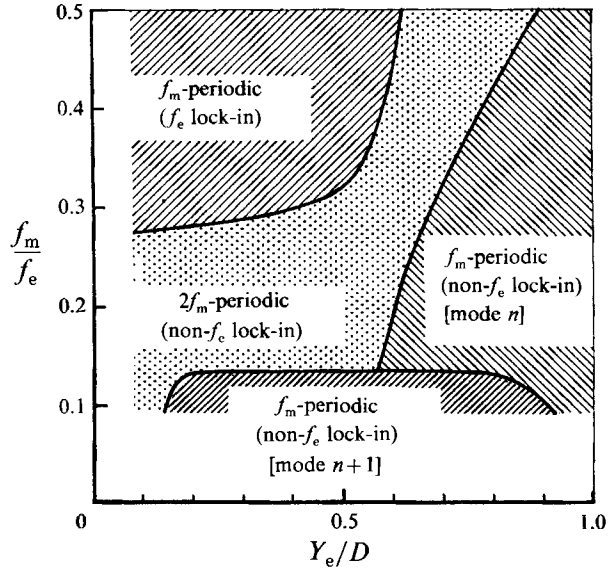

FIGURE 3. States of response of near wake as function of dimensionless modulation frequency f_m/f_e and amplitude Y_e/D at $f_e/f_0^* = 0.95$.

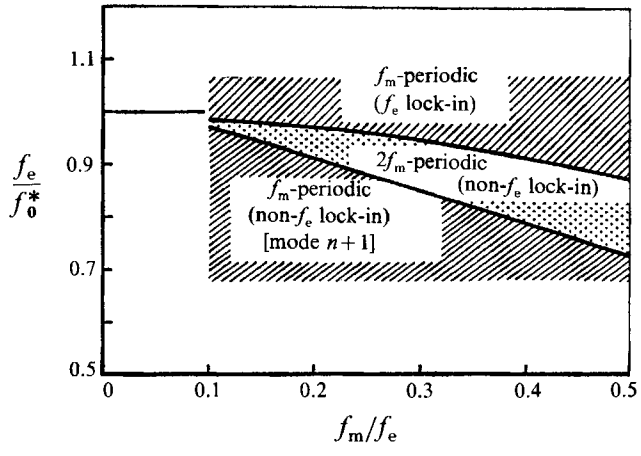

FIGURE 4. Effects of nominal excitation frequency f_e/f_0^* and modulation frequency f_m/f_e on states of response of near wake at $Y_e/D = 0.5$.

response defined in figure 3. At sufficiently high nominal frequency f_e/f_0^*, only the f_m periodic response with f_e lock-in occurs. Conversely, at sufficiently low f_e/f_0^* only the f_m periodic response with non-f_e lock-in occurs over the entire range of modulation frequency f_m/f_e. As the value of f_m/f_e increases, the band of the $2f_m$ periodic response increases. We therefore conclude that in order to induce a low-order chaotic response of the near wake, it is necessary to detune slightly the system from the matched excitation frequency $f_e/f_0^* = 1.0$. Slight detuning, in fact, is the focus of the present investigation, which concentrates on the representative case $f_e/f_0^* = 0.95$. This case is particularly significant in that it represents a highly locked-in response of the wake for purely sinusoidal excitation, thereby providing a well-defined reference case for amplitude-modulated excitation.

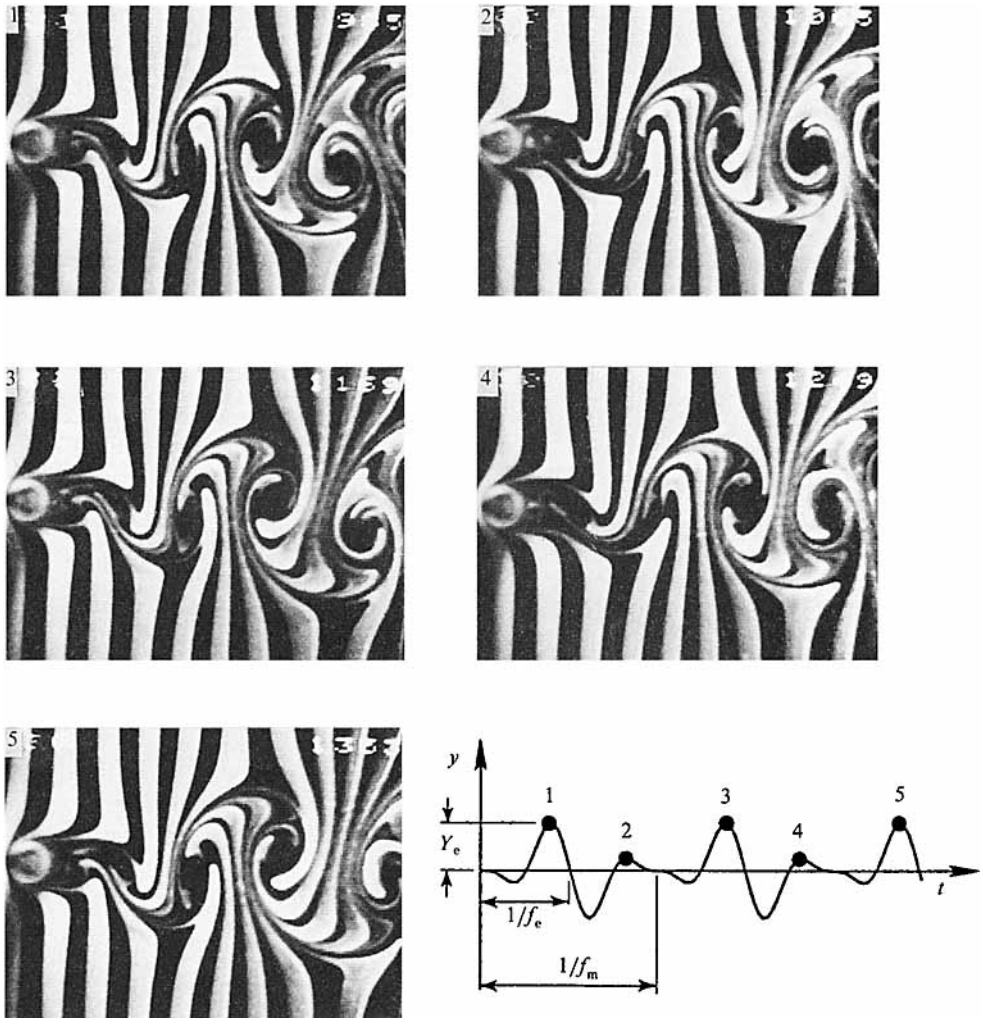

FIGURE 5. Visualization of vortex patterns in near wake for locked-in state of response. $f_m/f_e = 1/2$, $f_e/f_0^* = 0.95$, $Y_e/D = 0.2$.

In the following, we address the details of the vortex patterns and the velocity spectra associated with the regimes defined in figure 3.

4. Locked-in response of the wake (f_m cycle periodic with f_e lock-in)

This regime of response, represented by the schematics of figures 2(*a*) and 2(*b*) and the upper left domain of figure 3, corresponds to periodicity at frequency f_m and lock-in of the vortex pattern from one f_e cycle to the next. As illustrated in the photo layout of figure 5, the flow structure in the very near wake is repetitive in photos 1, 3 and 5; moreover, it is also repetitive in photos 2 and 4. These two sets of photos correspond respectively to the maximum and minimum peak amplitudes during f_m modulation. There is actually little distinction between the left and right columns of photos in figure 5. The principal difference occurs in the very near-wake formation region immediately behind the cylinder, where the formation of the first vortex from

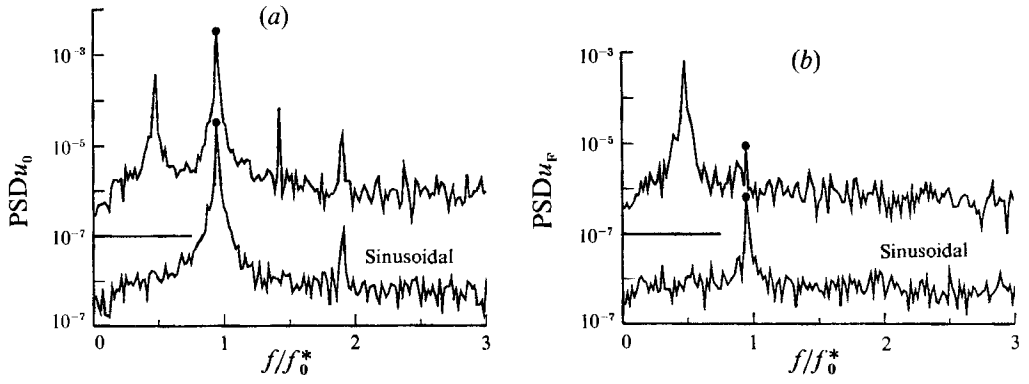

FIGURE 6. Spectra representing (*a*) near- and (*b*) far-wake regions for locked-in state of wake. $f_m/f_e = 1/2$, $f_e/f_0^* = 0.95$, $Y_e/D = 0.2$.

the lower side is particularly evident for cycles 1, 3 and 5; on the other hand, the first vortex is from the upper side of the cylinder in photos 2 and 4.

Comparison of the velocity spectra in the near- and far-wake locations is given in figure 6 for the cases of purely sinusoidal excitation and amplitude-modulated (AM) excitation. In all spectra, the solid dot represents the nominal excitation frequency. In the near wake, the spectrum corresponding to amplitude-modulated excitation shows a resonant, sharply peaked response at the nominal (carrier) frequency f_e and the sidebands $f_m = \pm\frac{1}{2}f_e$. In the far wake, the amplitude of the purely sinusoidal response has been attenuated by nearly two orders of magnitude relative to its near-wake value, while the lower sideband f_m has grown to a value that overshadows the excitation frequency component at f_e by three orders of magnitude.

The mechanisms associated with the transformation of these spectra are illustrated in the photos of figure 7. The dimensions of each photo are $20D$ in streamwise direction and $15D$ in the cross-streamwise direction. As a reference, the lower row of photos shows the response to purely sinusoidal forcing at the streamwise locations $x/D = 5$, 20, and 35. The wavelength of the vortex street remains essentially the same, suggesting that the frequency is nearly invariant. However, the rate of rollup of the timeline pattern due to the vortical structures decreases with increasing streamwise distance, indicating that the circulation of the vortices is decreasing as well (Gursul, Lusseyran & Rockwell 1990). This observation is in accord with the streakline investigation of Cimbala, Nagib & Roshko (1988), who demonstrated the trend towards disappearance of vortical structures at larger values of x/D due to viscous diffusion of vorticity. This apparent decrease in circulation agrees with the substantial decrease in the amplitude of the peak at excitation frequency f_e in the spectrum of figure 6. The case of AM excitation is indicated in the top two rows of photos. Photos in the second row are delayed by a time $1/f_m$ relative to those at $t = 0$, in order to illustrate the degree of repeatability. At $x/D = 5$, the vortex pattern is similar to that of purely sinusoidal forcing. At $x/D = 20$ and 35, the vortex street retains its structure at period $1/f_m$ while undergoing substantial distortion leading to an increase in wavelength between the principal vortical structures. It is this distortion that yields predominance of the lower-sideband component $f_m = \frac{1}{2}f_e$ in the spectrum of figure 6. The predominance of these large-scale structures in the downstream regions of the wake is, of course, compatible with the increasing width of the mean wake. Cimbala *et al.* (1988) emphasize, for the case of a wake not subjected to forced excitation, that the appearance of large-scale structures at larger

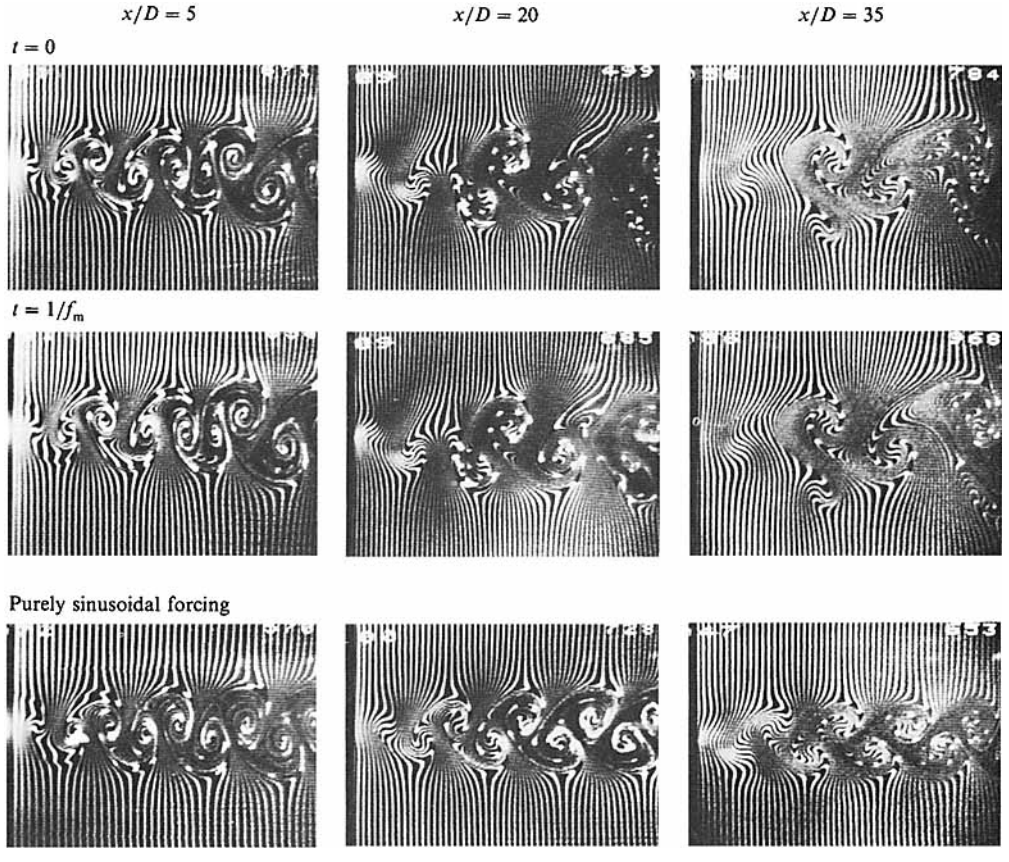

FIGURE 7. Streamwise evolution of wake corresponding to locked-in state of near wake. $f_m/f_e = 1/2$, $f_e/f_0^* = 0.95$, $Y_e/D = 0.2$. Streamwise distance x is distance from centre of cylinder; D is cylinder diameter.

streamwise distances is driven by the hydrodynamic instability of the local mean flow, and the vortex–vortex amalgamations accompanying the appearance of the larger structures is incidental. In the present case of forced excitation, the lower-frequency sideband component survives the streamwise evolution of the wake; it is most compatible with the local lengthscale of the mean wake. Conversely, the upper-sideband component is incompatible.

The principal feature of this regime of response due to AM excitation is therefore to filter out all spectral components except that corresponding to the lower sideband, or in other words, the f_m component. In the field of electronics, this suppression, or removal, of the carrier signal at f_e and retention of only a single sideband component at f_m produces a single-sideband, suppressed-carrier AM signal. The time signal corresponding to the far-wake spectrum of the AM case in figure 6 corresponds to this sort of suppression of the carrier signal. From an electronics standpoint, this suppressed-carrier signal can be produced by what is known as a double-balanced modulator (Goodyear 1971). The fluid mechanical analogy involves distortion and merging of adjacent vortical structures in the manner shown in figure 7.

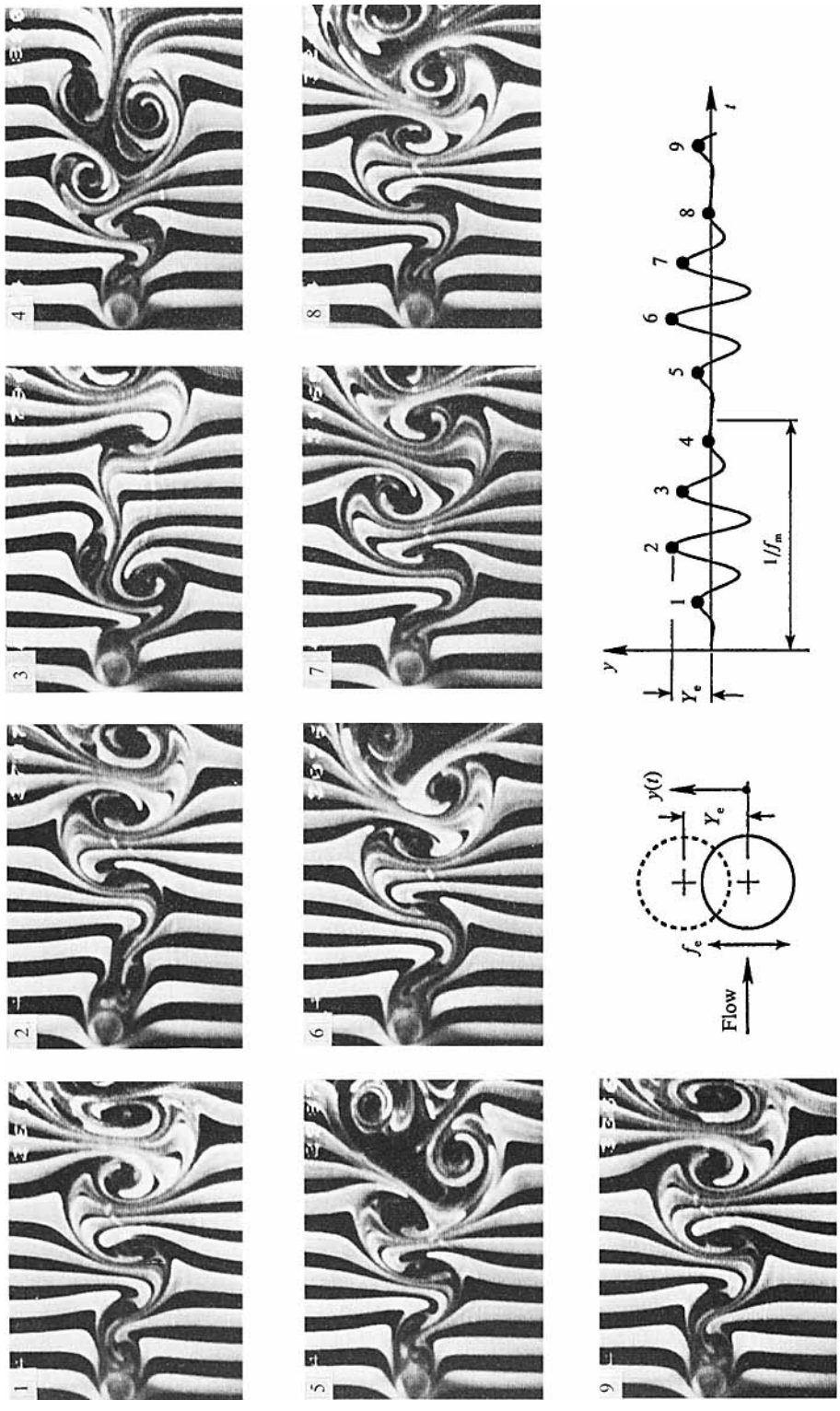

FIGURE 8. Visualization of period-doubled state of response of wake, $f_m/f_e = 1/4$, $f_e/f_0^* = 0.95$, $Y_e/D = 0.5$.

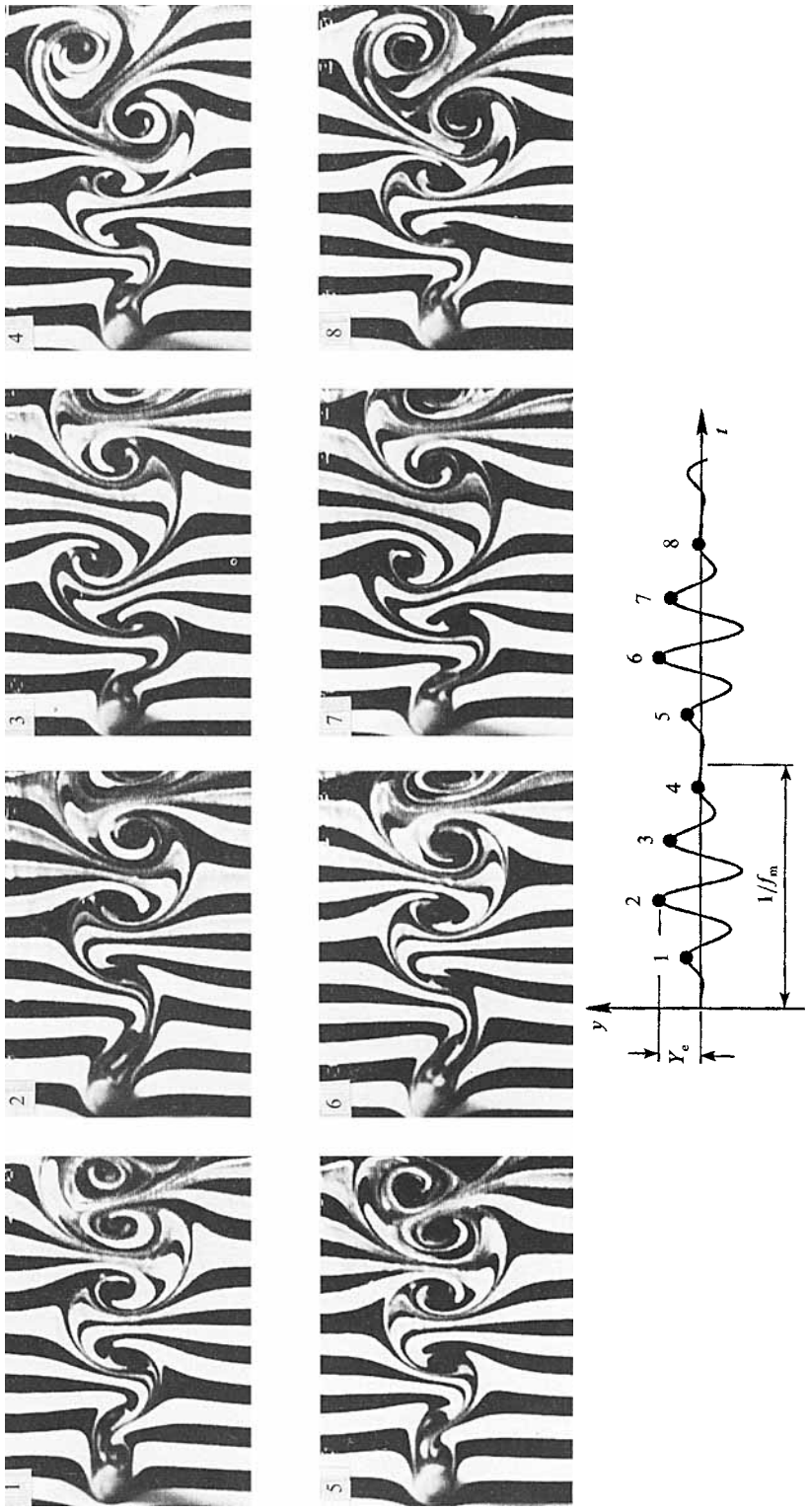

FIGURE 9. Visualization of locked-in state of response of wake obtained by retuning nominal excitation frequency to the value of $f_e/f_0^* = 1.0$ from the 0.95 in figure 8. $f_m/f_e = 1/4$, $Y_e/D = 0.5$.

5. Period-doubled response of the wake ($2f_m$ periodic)

This regime of response represents a period-doubled version of the f_m periodic regime described in the previous section. The nature of this period doubling was described in figure 2(*c*), which gives a simplified schematic of a typical $2f_m$ periodic response.

Corresponding flow visualization for the $2f_m$ periodic response is given in figure 8. The two f_m cycles include photos 1–8. The flow structure is essentially the same in photos 1 and 9 extending over a total time period of $2/f_m$. During the first f_m cycle, extending from photos 1–4, the flow structure undergoes substantial alteration. Moreover, the initially formed vortex switches from the bottom side of the cylinder in photo 1 to the top side in photo 3. We therefore witness a dephasing of the initially formed vortex relative to the cylinder motion and consequently severe alterations of the downstream vortex street. During the second f_m cycle, extending from photos 5–8, the flow structure is qualitatively similar and the initially formed vortex in the very near wake is unaltered, owing to the occurrence of lock-in during each f_e cycle.

The response of the near-wake can be retuned to a locked-in state by slightly increasing the nominal excitation frequency to $f_e/f_0^* = 1.0$, while holding all other parameters constant. The visualization photos of figure 9, taken at two comparable instants during two successive cycles, show a highly repetitive flow structure. This concept of a locked-in response at $f_e/f_0^* = 1.0$ does, in fact, hold for the whole range of f_m/f_e and Y_e/D considered herein. Detuning to $f_e/f_0^* \neq 1.0$ is necessary in order to induce destabilization of the near wake.

A comparison of the vortex patterns of figures 8 and 9 at the peak amplitude 3 shows a large difference in the basic structure; the same observation holds in comparing the structure at peak amplitude 4. On the other hand, the same type of comparison between figures 8 and 9 for peak 7, then peak 8, shows a qualitatively similar structure. Recall that at $f_e/f_0^* = 0.95$ (figure 8), non-f_e lock-in occurs during the first part of the $2f_m$ cycle; correspondingly, at $f_e/f_0^* = 1$ (figure 9), lock-in occurs. This explains the difference in the flow structure between $f_e/f_0^* = 0.95$ and 1.0 at these instants during the oscillation cycle. Moreover, at $f_e/f_0^* = 0.95$, f_e lock-in occurs during the second part of the $2f_m$ cycle; correspondingly, at $f_e/f_0^* = 1.0$, f_e lock-in also occurs. This observation explains the similarity of the response at $f_e/f_0^* = 0.95$ and 1.0 over this portion of the cycle. In essence, the slight detuning of the nominal excitation frequency f_e/f_0^* can generate substantially different vortex patterns in the near wake due to the onset of a period-doubled $2f_m$ periodic response.

The velocity spectra for this $2f_m$ periodic response are given in figure 10(*a*). In the near-wake, the background (broadband) level is high at low frequencies; however, there are sharp spectral peaks corresponding to five of the seven $2f_m$ sidebands below the nominal excitation frequency. In the far wake, this initial destabilization has led to a rapid broadening of the spectrum; the peak value is an order of magnitude higher than that of the corresponding sinusoidally perturbed wake. The case of the wake that has been retuned to a lock-in state is represented by the spectra in figure 10(*b*). In the near wake, the amplitudes of the f_m modulation sidebands rise well above the background (broadband) level; moreover, the background level is lower than that at $f_e/f_0^* = 0.95$. In the far wake, for $f_e/f_0^* = 1$, the background level over the lower range of frequency is substantially lower than that corresponding to $f_e/f_0^* = 0.95$. Furthermore, the two lowest sideband components at $f_e/f_0^* = 1.0$ are well defined in comparison with their counterparts at $f_e/f_0^* = 0.95$.

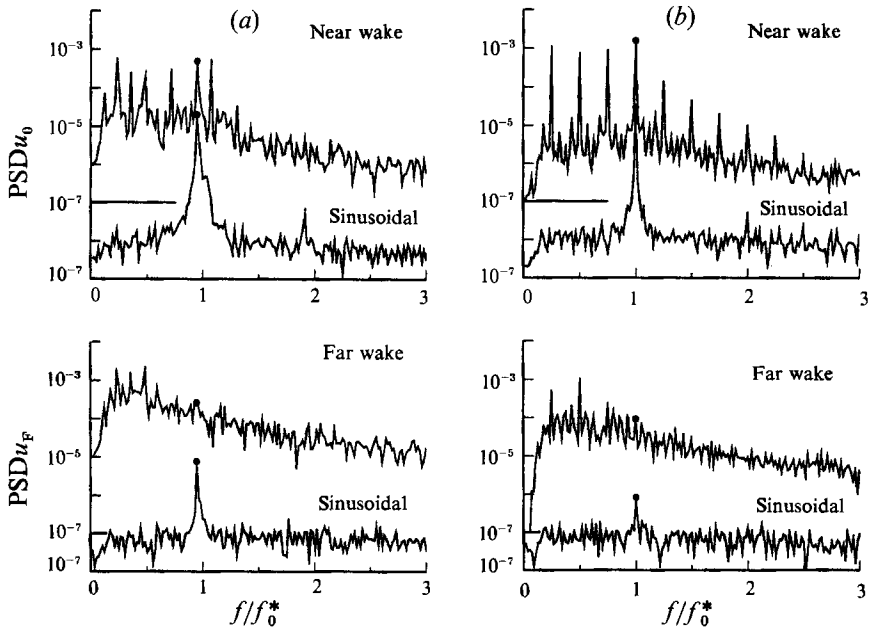

FIGURE 10. (*a*) Spectra showing response of near- and far-wake regions for period-doubled state of response of near-wake. $f_m/f_e = 1/4$, $f_e/f_0^* = 0.95$, $Y_e/D = 0.5$. (*b*) spectra showing lock-in state of near-wake and corresponding far-wake spectra for nominal excitation frequency retuned to $f_e/f_0^* = 1.0$ for same modulation parameters as in (*a*).

The evolution of the $2f_m$ periodic wake in the downstream direction is illustrated in figure 11. At $x/D = 5$, the vortex pattern is unrepeatable at instants corresponding to $t = 0$ and $1/f_m$. On the other hand, the patterns at $t = 0$ and $2/f_m$ are essentially identical, indicating the $2f_m$ periodicity. The photo at $t = 1/f_m$ shows that clusters of small-scale interacting vortices are interspersed among large-scale vortical structures as a result of the near-wake modulation process. At $x/D = 35$, the nature of the large-scale vortex pattern exhibits a substantial change from one f_m cycle to the next; it is not repetitive at $t = 2/f_m$, meaning that the well-defined period doubling present in the near wake has given way to a relatively disorganized response at this location in the downstream wake. This trend corresponds to the increase of the broadband, low-frequency energy in the far-wake spectrum in figure 10(*a*). These large-scale patterns at $x/D = 35$ contrast with the case where there is purely sinusoidal forcing, for which small-scale, highly organized vortex patterns are barely discernible.

The $2f_m$ periodic response also can be attained at very high f_m/f_e, provided the amplitude Y_e/D is large. The photo layout of figure 12 illustrates the typical wake structure. It emphasizes the $2f_m$ periodicity over two successive $2f_m$ cycles. Irrespective of which instant during the oscillation cycle of the cylinder is selected, the pattern is always repetitive with a time delay $2/f_m$, and there are severe distortions of the vortex street from its classical form. The general nature of the near-wake response is the same as that illustrated in figure 8, with destabilization of the initially formed vortex over the first portion of the $2f_m$ cycle and stable formation over the second portion. As for the case of figure 8, the system can be retuned to a stable, locked-in response by slightly raising the nominal excitation frequency f_e/f_0^* to a value of 1.00. The vortex patterns corresponding to this case are illustrated in

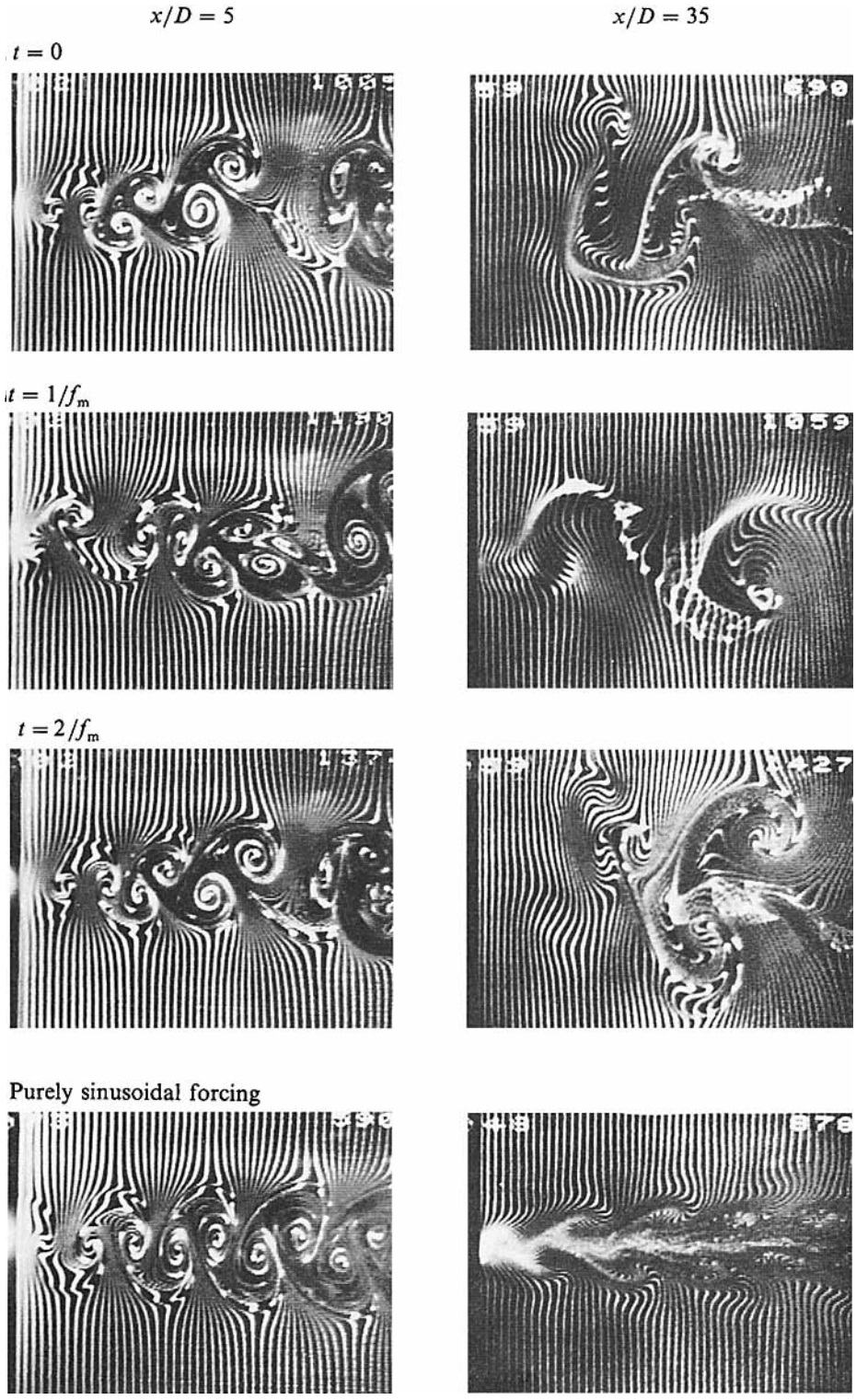

FIGURE 11. Visualization of streamwise evolution of wake for period-doubled state of response, at $f_m/f_e = 1/4$, $f_e/f_0^* = 0.95$, and $Y_e/D = 0.5$. Corresponding case of purely sinusoidal forcing is also illustrated.

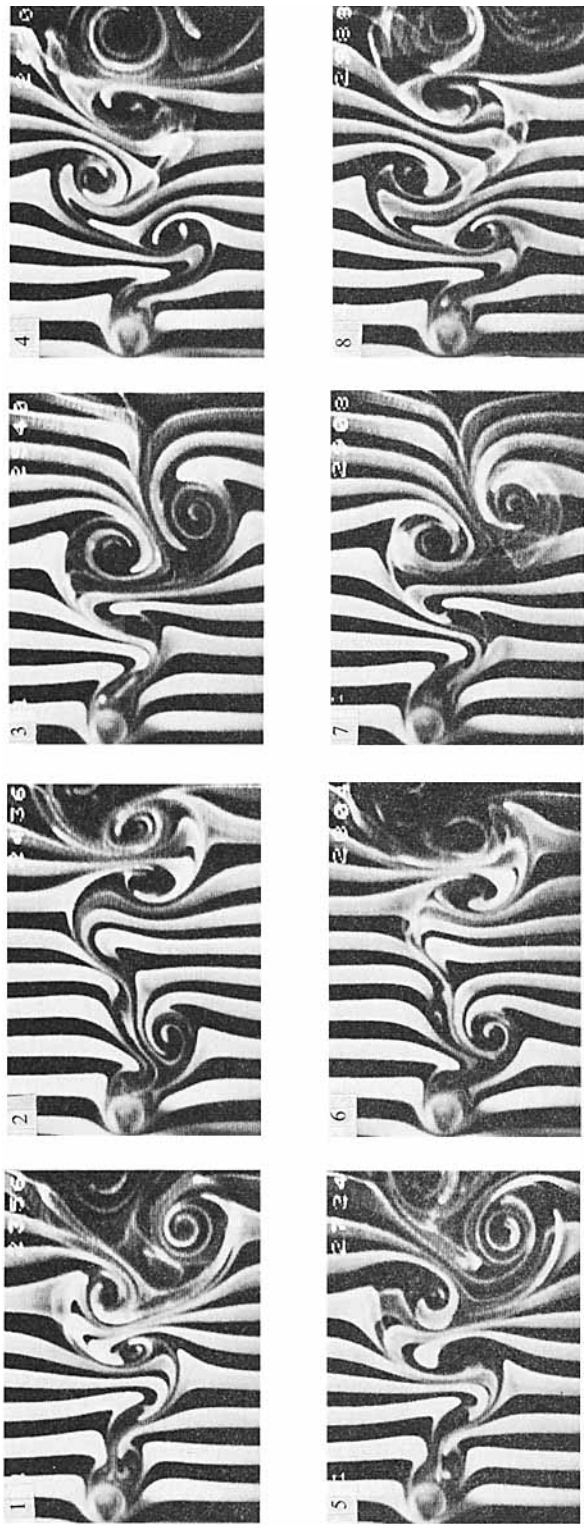

FIGURE 12. Period-doubled state of response: $f_m/f_e = 1/2$, $f_e/f_0^* = 0.95$, and $Y_e/D = 0.8$.

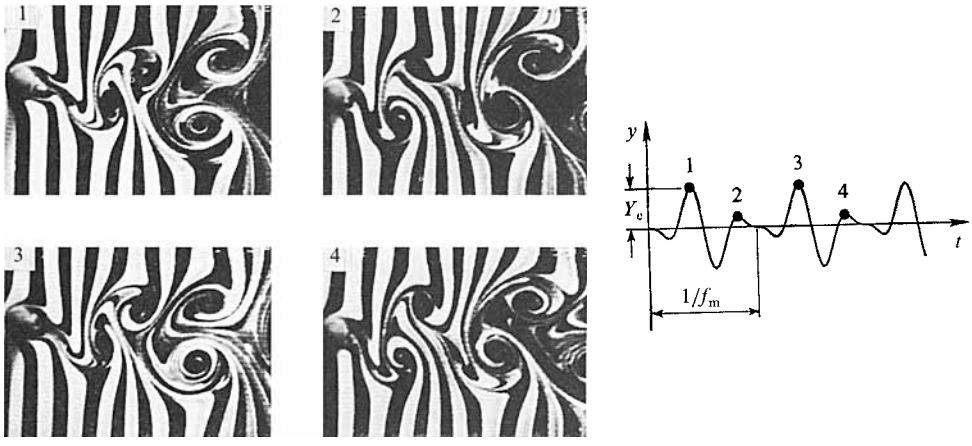

FIGURE 13. Locked-in state of response attained by retuning nominal excitation frequency to $f_e/f_0^* = 1.0$ from the condition of figure 12. $f_m/f_e = 1/2$, $Y_e/D = 0.8$.

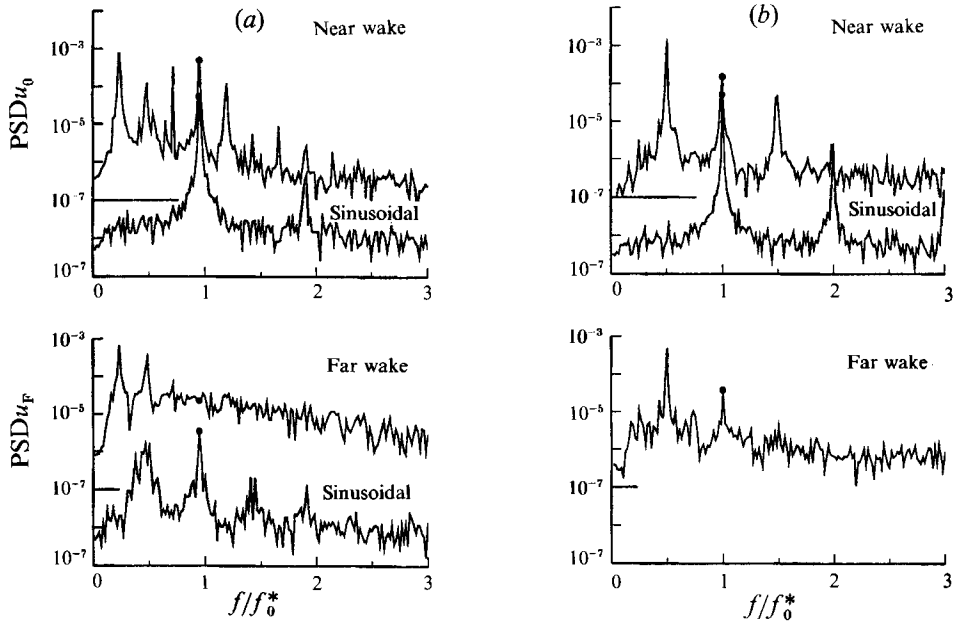

FIGURE 14. Spectra showing response of near- and far-wake regions for (*a*) period-doubled state and (*b*) locked-in state of near-wake response corresponding respectively to values of nominal excitation frequency $f_e/f_0^* = 0.95$ and 1.0. $f_m/f_e = 1/2$, $Y_e/D = 0.8$.

figure 13. The basic form of the classical vortex street is retained, although it is somewhat distorted due to the very large amplitudes.

Velocity spectra corresponding to the $2f_m$ periodic response of figure 12 are given in figure 14(*a*). As for the previous case of $2f_m$ modulation, shown in figure 10(*a*), the background (broadband) level at low frequencies is high, but discrete, large-amplitude peaks are evident. The three lower sidebands correspond to the period-doubled response. On the other hand, only the first upper sideband has a large amplitude. In the far wake, there occurs substantial spectral broadening in the same spirit as for the previous cases of destabilized flows, except that the lower two

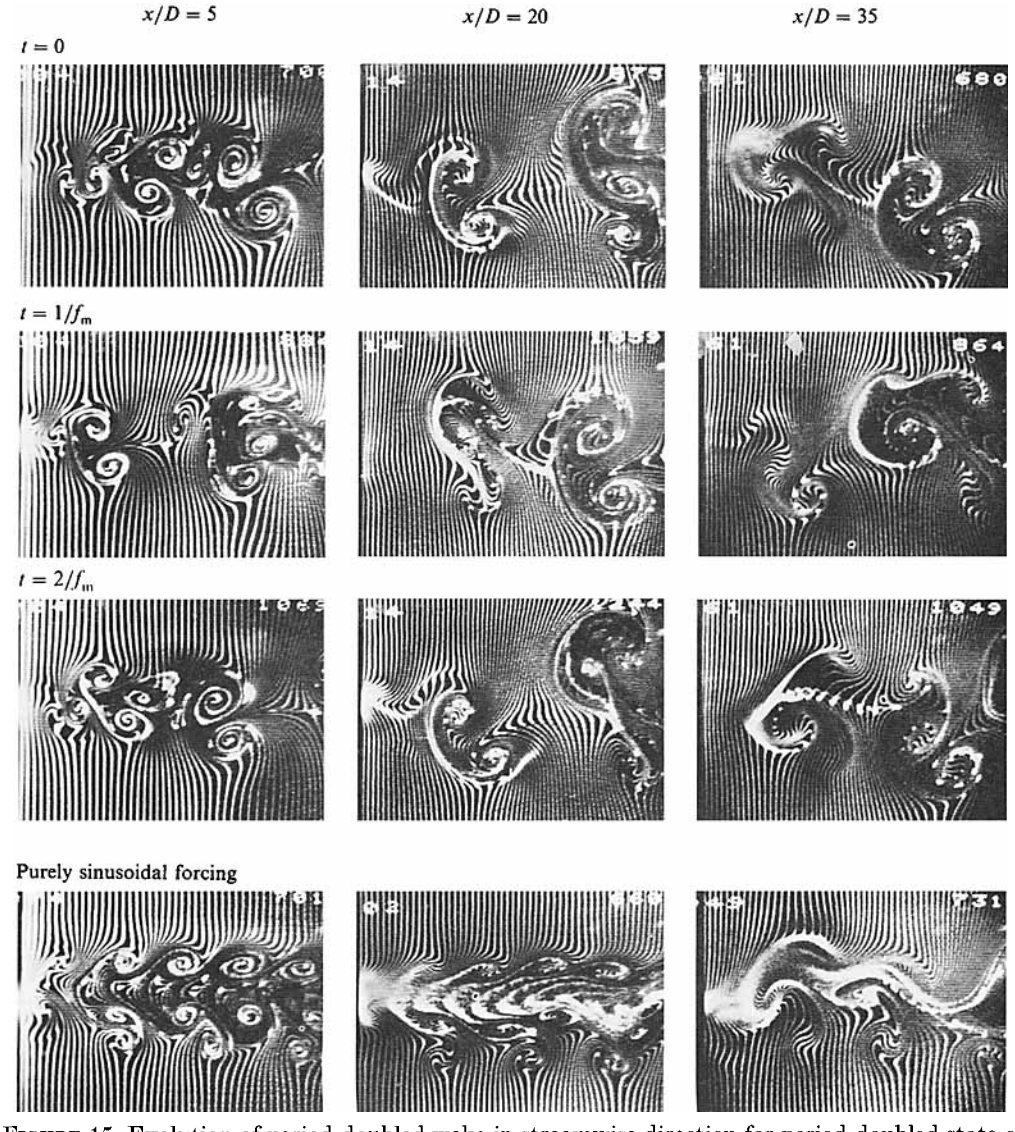

FIGURE 15. Evolution of period-doubled wake in streamwise direction for period-doubled state of response of near wake. $Y_e/D = 0.8$, $f_e/f_0^* = 0.95$, $f_m/f_e = 1/2$. Corresponding case of purely sinusoidal forcing is also shown.

sidebands survive the spectral broadening process. This sort of filtering out, or suppression, of all spectral components except the lowest one or two sideband components is characteristic of the wake response at high values of modulation frequency f_m/f_e, even at considerably lower values of amplitude. The case of the locked-in near wake at $f_e/f_0^* = 1$ is shown in figure 14(*b*). The lower sideband at f_m dominates the spectra; this dominance extends to the far wake. Moreover, the amplitude level of the broadband, background fluctuations is substantially reduced relative to that of $f_e/f_0^* = 0.95$.

The streamwise evolution of the wake corresponding to the photos of figure 12 and the corresponding spectra of figure 14(*a*) is shown in the photo layout of figure 15. At $x/D = 5$, the vortex pattern nearly repeats at $t = 0$ and $t = 2/f_m$. Comparing this

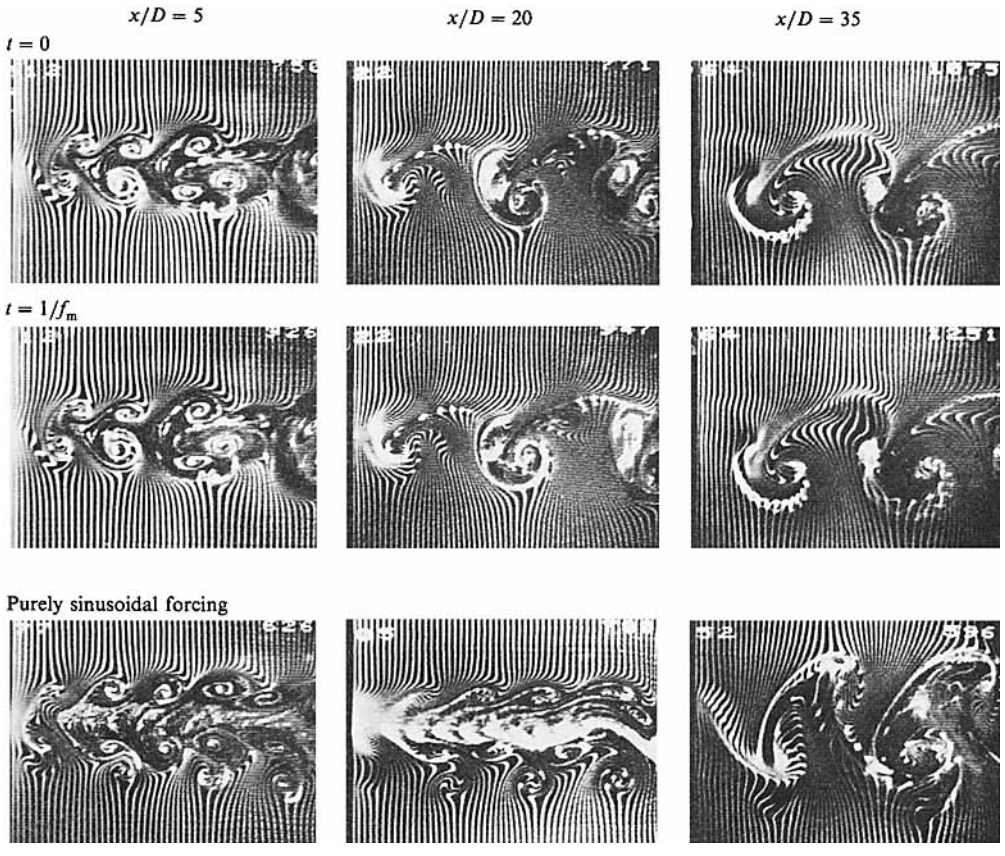

FIGURE 16. Streamwise evolution of wake corresponding to locked-in state of near wake attained by retuning nominal excitation frequency to $f_e/f_0^* = 1.00$ from $f_e/f_0^* = 0.95$ shown in figure 15. $f_m/f_e = 1/2$, $Y_e/D = 0.8$. Also illustrated in case of purely sinusoidal forcing.

pattern with that at $t = 1/f_m$, it is evident that the wake involves isolated clusters of interacting small-scale vortices travelling in the streamwise direction. The consequence of these interactions is to produce large-scale vortical structures, evident at $x/D = 20$. Further downstream, at $x/D = 35$, the large-scale vortices are still identifiable, and there is a degree of repetition in the patterns at $t = 0$ and $2/f_m$. For the corresponding case of purely sinusoidal forcing, shown in the bottom row of photos of figure 15, at $x/D = 5$, counter-rotating vortex pairs are formed in the bottom row of the vortex street (Williamson & Roshko 1988), while a single row of vortices of like sense are generated in the top row. Sufficiently far downstream at $x/D = 35$, this configuration exhibits a long-wavelength, low-frequency instability with identifiable coherent vortical structures along the bottom of the wake. This process is associated with the appearance of the relatively large-amplitude sub-harmonic component in the corresponding spectrum of figure 14.

The evolution of the wake for the same conditions of AM excitation, but for retuning to $f_e/f_0^* = 1.0$, is illustrated in figure 16. The vortical structures are highly repetitive, even at the largest streamwise distance $x/D = 35$. Moreover, for the corresponding case of purely sinusoidal excitation, the occurrence of well-defined structures at $f_m = \frac{1}{2}f_e$ contrasts with sinusoidal excitation at $f_e/f_0^* = 0.95$ shown in figure 15.

6. Fully destabilized response of the wake (f_m periodic with non-f_e lock-in – mode $n+1$)

As represented by the regime at the bottom of figure 3, this type of response exists over a relatively wide range of amplitude Y_e/D provided that the dimensionless modulation frequency f_m/f_e is sufficiently low. Figures 17, 18 and 19 represent the near-wake flow structure at the same value of modulation frequency, but successively larger amplitudes of oscillation. At the lowest amplitude, depicted in figure 17, the patterns of vortical structures are nearly mirror images, or inversions of one another, at the indicated instants during the initial and final stages of the f_m cycle, represented by the following pairs of photos: 1 and 5; 2 and 6; 3 and 7; 4 and 8; these inversions of the vortex pattern suggest a time-varying *phase modulation* of the near-wake structure, relative to the cylinder displacement, during the course of the f_m cycle. In fact, if one examines the very first small-scale vortex formed from the cylinder, it is from the upper shoulder in photos 2–4 and from the lower shoulder of the cylinder in photos 6–8. Photos 9 and 1 are essentially the same, indicating that these continuous phase changes during an f_m cycle lead to a return to the original vortex pattern and the original timing of the initial vortex formation at the end of each f_m cycle. As was illustrated in the schematic of figure 2(*e*), this particular regime of response adds one vortex pair per f_m cycle of oscillation beyond the $n = f_e/f_m$ vortex pairs that would exist in the case of f_e cycle lock-in. This addition of the vortex pair is related to the inversion of the vortex patterns in the pairs of photos: 1 and 5; 2 and 6; and so on. This pattern can be deduced by comparing the visualization of figure 17 with the representation of figure 2(*e*), which is valid for the range of amplitudes in this particular regime of response.

At a larger amplitude of excitation, represented by the photos in figure 18, the near-wake structure exhibits substantial distortions from one f_e cycle to the next during the course of the f_m modulation period. The principal feature is production of small-scale, interacting vortices, evident in photos 4–6. The flow structure returns to its original pattern at the end of the f_m cycle, evident by comparing photos 9 and 1. We again witness a continuously changing phase of the initially formed vortex from cycle to cycle of the cylinder motion; in photos 3 and 4, for example, the initially formed vortex is from the upper side of the cylinder, while in photos 7 and 8 it is from the lower side.

At the highest amplitude, represented in figure 19, the vortex arrangement passes through a series of patterns involving generations of small-scale vortices, followed by larger-scale vortices that are thrust outwards away from the centreline of the cylinder. Photos 1 and 9 evidence the repetition of the flow structure with period $1/f_m$. No single photo taken during the course of this f_m cycle replicates the pattern associated with purely sinusoidal forcing, shown at the lower right of figure 19. It involves formation of counter-rotating vortex pairs on one side of the vortex street, as defined by Williamson & Roshko (1988). Concerning the initially formed vortex, it is clearly from the upper side of the cylinder in photo 3 and from the lower side in photos 5 and 6, again indicating a continuous variation of the phase shift between the vortex formation and the cylinder motion during the course of an f_m cycle.

Irrespective of the particular pattern of vortex formation shown in figures 17–19, a central feature is the phase modulation, or continuous variation of phase of the initially formed vortex. These observations suggest that employment of low values of modulation frequency f_m/f_e effectively destabilizes what would normally be a phase-locked response of the near-wake structure in the case of purely sinusoidal

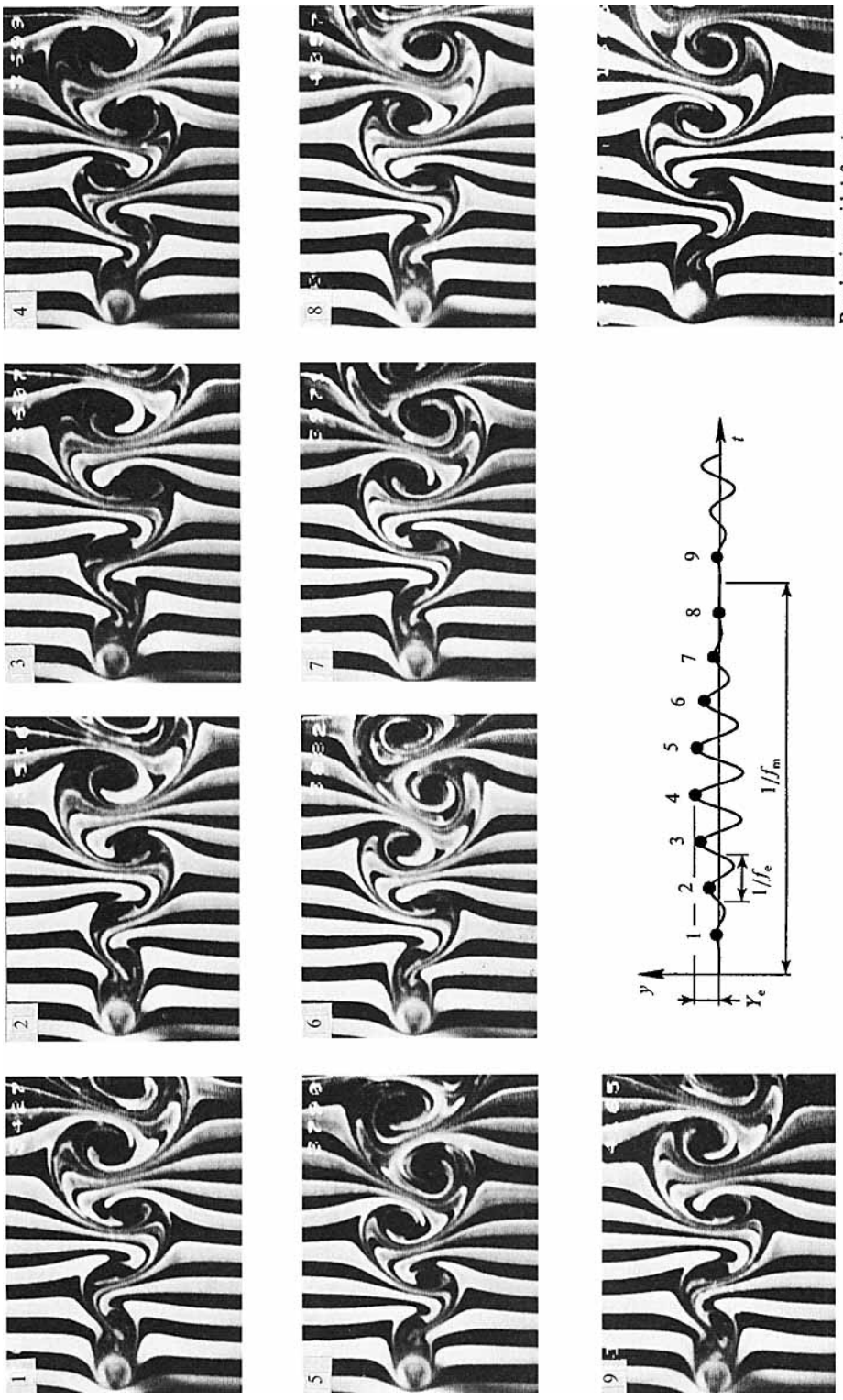

FIGURE 17. Fully destabilized state of response of near wake at low excitation amplitude. $f_m/f_e = 1/8$, $f_e/f_0^* = 0.95$, $Y_e/D = 0.2$.

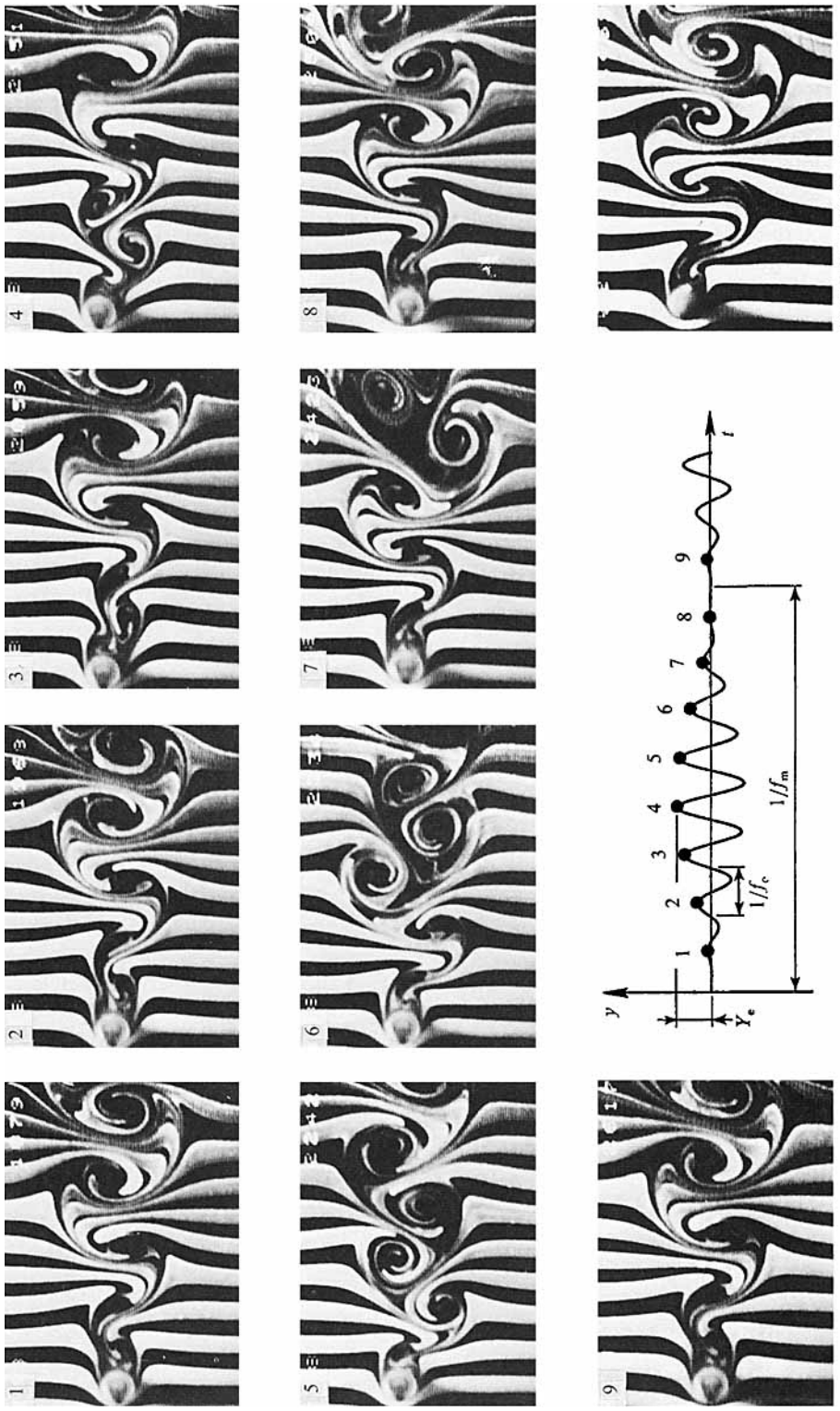

FIGURE 18. Fully destabilized state of response of near-wake at moderate excitation amplitude. $f_m/f_e = 1/8, f_e/f_0^* = 0.95, Y_e/D = 0.5$.

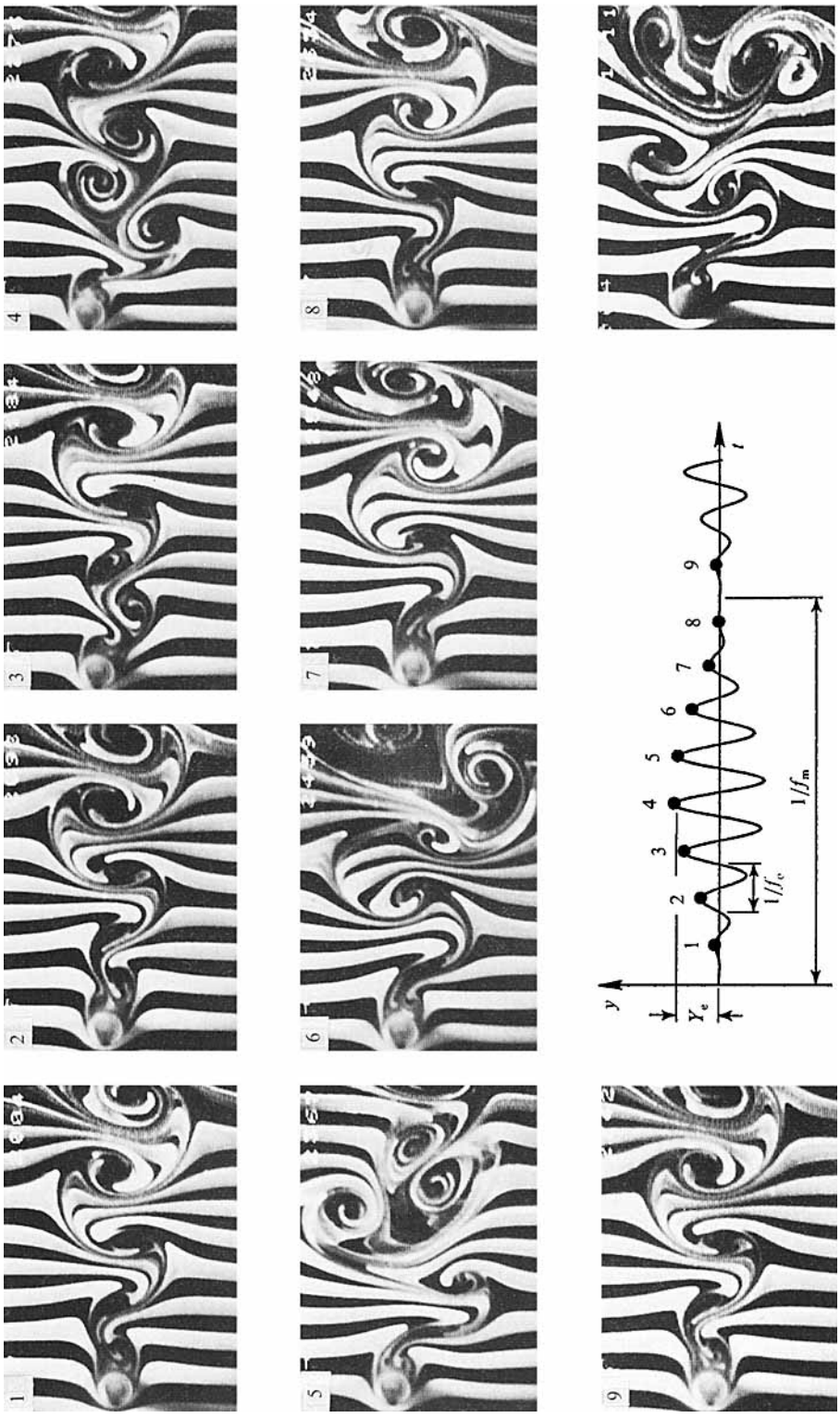

FIGURE 19. Fully destabilized response of near wake at large excitation amplitude. $f_m/f_e = 1/8$, $f_e/f_0^* = 0.95$, $Y_e/D = 0.8$.

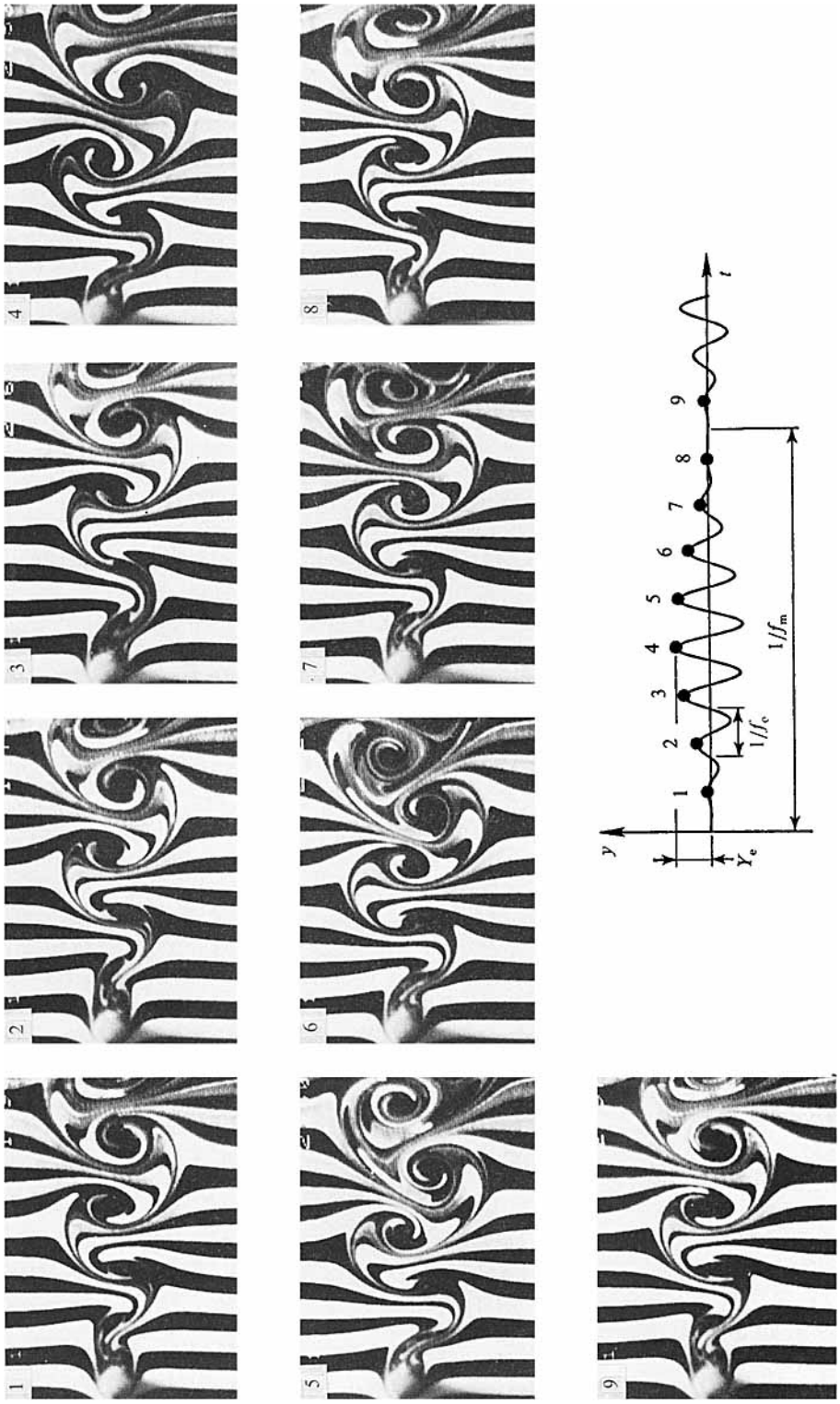

FIGURE 20. Locked-in state of response of near-wake obtained by retuning nominal excitation frequency to $f_e/f_0^* = 1.00$ from $f_e/f_0^* = 0.95$ in figure 18. $f_m/f_e = 1/8$, $f_e/f_0^* = 1.00$, $Y_e/D = 0.5$.

excitation. For this destabilization to occur, however, the nominal excitation frequency f_e/f_0^* must be detuned from the matched excitation condition, $f_e/f_0^* = 1.0$, as already suggested for the other categories of wake response described in the foregoing. This concept is dramatically illustrated by the flow visualization sequence of figure 20 corresponding to $f_e/f_0^* = 1.0$, and acquired for exactly the same excitation conditions as for the AM excitation of figure 18 at $f_e/f_0^* = 0.95$. Not only are the initially formed vortices essentially phase-locked from one f_m cycle to the next, but the patterns of vortex formation are substantially different than those of figure 18. For example, there are no clusters of small-scale vortices formed during the locked-in response of figure 20, and in fact, there is little deviation of the vortex patterns indicated therein from what one would expect from purely sinusoidal excitation. This locked-in response of figure 20 is represented by the schematic of figure 2(*a*).

The process of destabilization of the near wake, shown in figures 17–19, is expected to generate significantly different spectra, relative to that arising from purely sinusoidal excitation. This comparison is given in figure 21 for the range of amplitudes shown in figures 17–19. In the near-wake region, AM excitation substantially reduces the peak at the excitation frequency f_e relative to the case of purely sinusoidal excitation. Moreover, for all amplitudes, there is a substantial increase in the broadband, background level of the spectrum in the range of low frequencies. At the higher values of excitation amplitude, the lower f_m sidebands have a substantial amplitude and are superimposed on the high background level. In the far-wake region, it is evident that the destabilization process occurring in the near wake rapidly produces a broadband spectral response with a concentration of energy at the lowest values of frequency and complete suppression of the nominal excitation frequency f_e within the background spectrum.

For the same AM excitation conditions as at $Y_e/D = 0.5$, but for $f_e/f_0^* = 1.0$, the spectra take the form shown in figure 21(*d*). Very distinct spectral components representing the lower sideband f_m components exist not only in the near wake, but also in the far wake, suggesting that the initially induced lock-in state persists well downstream.

The streamwise evolution of the wake triggered by the destabilized near wake is illustrated in figure 22 for the case of moderate excitation amplitude ($Y_e/D = 0.5$). First of all, for the case of purely sinusoidal forcing, the timeline patterns at successive values of x/D shown in the bottom row of photos suggest that the predominant frequency induced in the near-wake region persists into the far wake. For the case of the wake subjected to AM excitation, shown in the first three rows of photos of figure 22, the flow structure at $x/D = 5$ is repetitive at $t = 0, 1/f_m$; these photos show that the merging of small-scale vortical structures is well underway. At $x/D = 20$, the vortex pattern is no longer repetitive at $t = 0$ and $t = 1/f_m$. The clustering of vortical structures on the right-hand side of these photos contrasts with the absence of vortical structures on the left-hand side. Such clusters, or groups, of vortices moving through the wake, are a basic feature of this type of modulation at low f_m/f_e. At $x/D = 35$, the time of appearance as well as the patterns of vortices is largely random. This irregularity of the wake is associated with the broadband spectrum of figure 21.

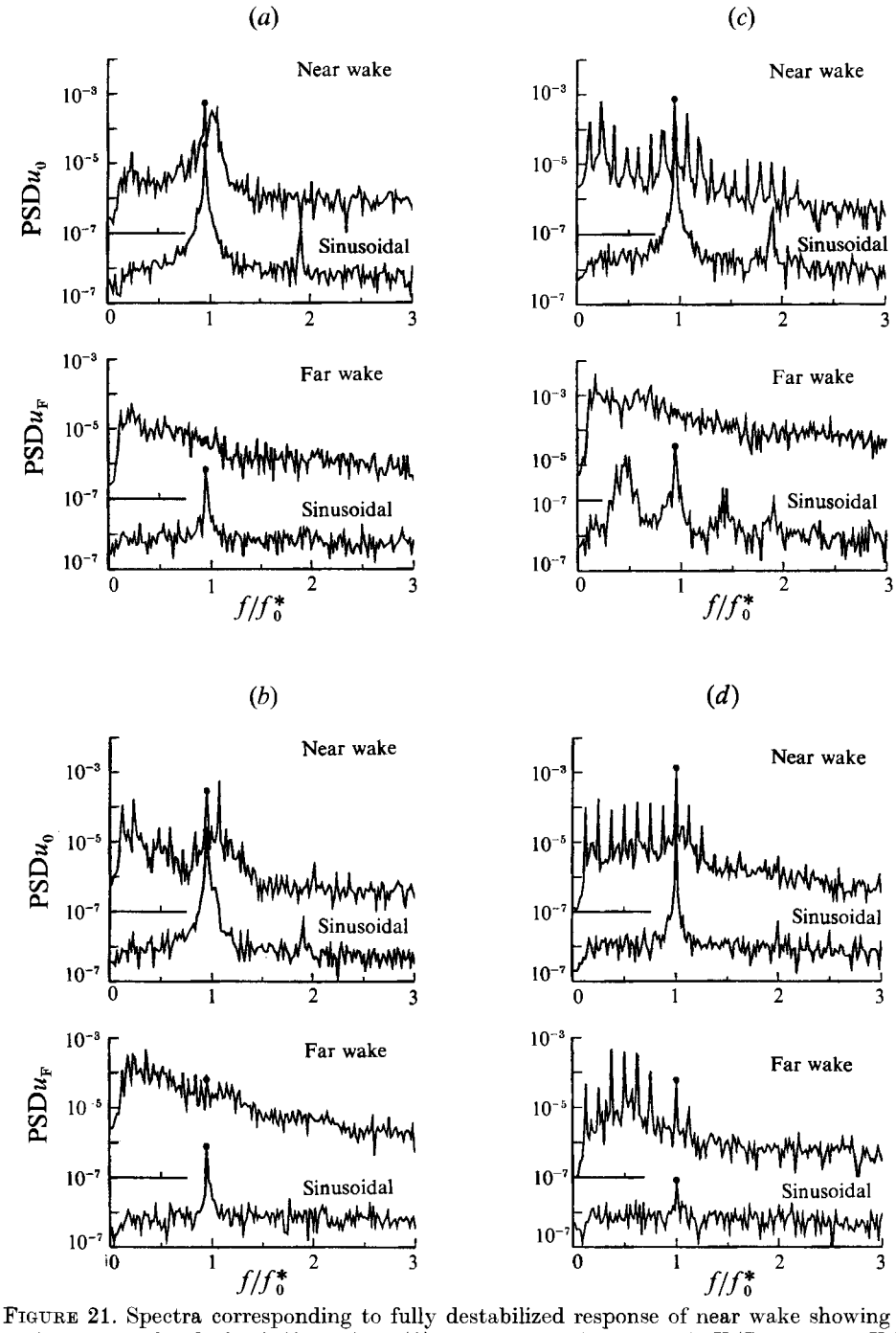

FIGURE 21. Spectra corresponding to fully destabilized response of near wake showing effect of excitation amplitude for $f_m/f_e = 1/8$, $f_e/f_0^* = 0.95$: (*a*) $Y_e/D = 0.2$; (*b*) $Y_e/D = 0.5$; (*c*) $Y_e/D = 0.8$. (*d*) The locked-in state of response obtained by retuning nominal excitation frequency to $f_e/f_0^* = 1.00$. $f_m/f_e = 1/8$, $Y_e/D = 0.5$.

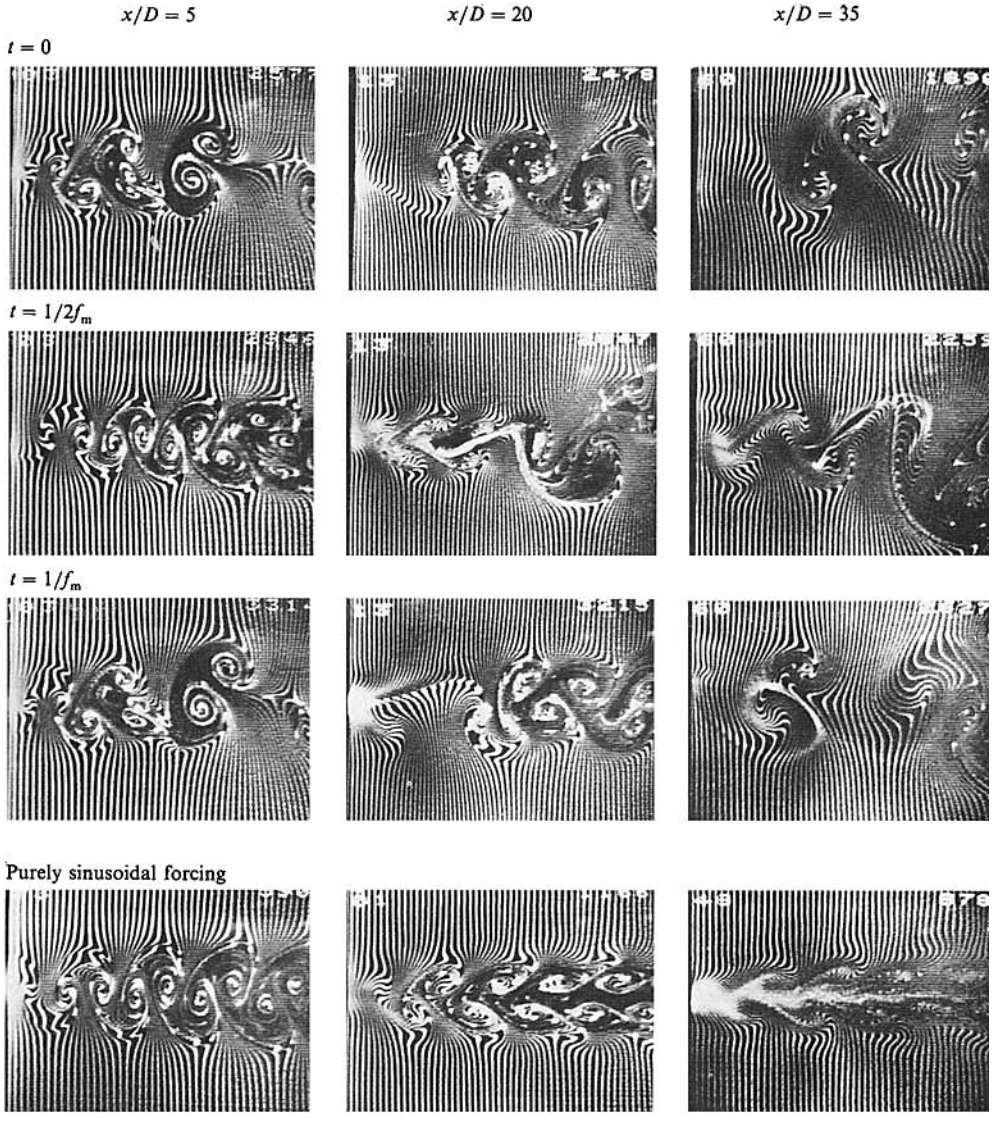

FIGURE 22. Streamwise evolution of flow structure of wake from fully destabilized state of near-wake response. $f_m/f_e = 1/8$, $f_e/f_0^* = 0.95$, $Y_e/D = 0.5$.

7. Fully destabilized response of the wake (f_m periodic with non-f_e lock-in – mode n)

As illustrated in figure 3, this type of f_m periodic response occurs at large amplitudes of the cylinder displacement Y_e/D and moderate values of modulation frequency f_m/f_e. The simplified schematic of figure 2 (d) represents the time evolution of the pattern of the near-wake vortices. Exactly $n = f_e/f_m$ pairs of vortices are formed per f_m cycle, but not in a repetitive or locked-in sense from one f_e cycle to the next. Figure 23 shows representative visualization of this regime of response. The lack of formation of a vortex having clockwise sense between peak amplitudes 1 and 2 in figure 2 (d) is eventually reflected in the right-hand side of photo 3 in figure 23. These vortex patterns are clearly repeatable from one f_m cycle to the next, evident

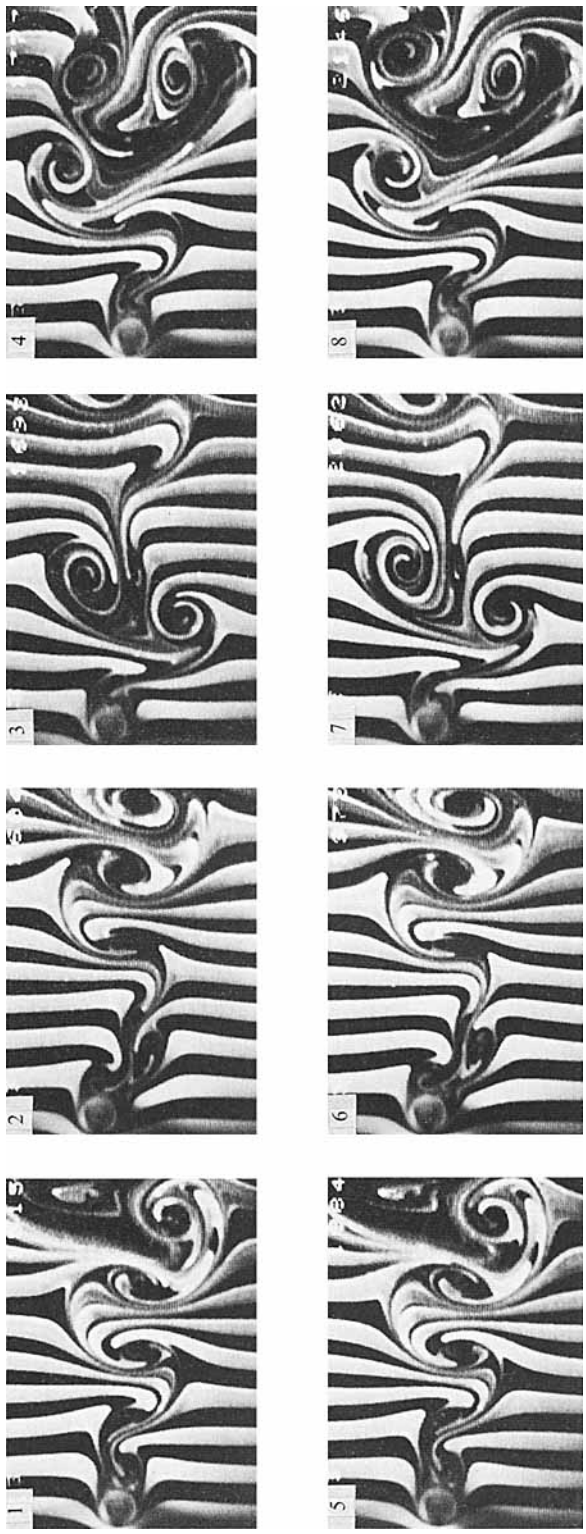

FIGURE 23. Fully destabilized state of response of near wake, $f_m/f_e = 1/4$, $f_e/f_0^* = 0.95$, $Y_e/D = 0.8$.

by comparing corresponding photos in the first and second rows of figure 23. There are, however, variations of the phase of the initially formed vortex from one f_e cycle to the next. It forms from the bottom side of the cylinder in photo 1, from the top at 2, and from the bottom again at 3. This sort of phase variation with time suggests a similar type of destabilization as for the $n+1$ mode discussed in §6. In fact, spectra acquired in the near wake (not shown here) exhibit a substantial increase in background level, upon which are superimposed the well-defined f_m sidebands. The spectrum has a very similar form to the corresponding case of figure 21. This sort of near-wake destabilization leads to rapid broadening of the spectrum in the downstream region of the wake, as was also observed for the category of wake response described in the preceding section.

8. Concluding remarks

The distinct states of response attainable by amplitude-modulated excitation can be categorized according to patterns of vortex rearrangement in the near wake, relative to the vortex pattern that is induced by purely sinusoidal excitation. The type of vortex rearrangement that is induced, and its phase relationship to the instantaneous displacement of the cylinder, has a strong influence upon the evolution of the wake in the downstream direction, and thereby the degree of organization in the far wake. Particularly remarkable is the fact that the near-wake vortex patterns are repeatable with a time delay $1/f_m$, designated as f_m periodic, or with a delay $2/f_m$, corresponding to its period-doubled version. Within this periodicity at f_m or $\frac{1}{2}f_m$, the vortex patterns can exhibit a locked-in response from one f_e cycle to the next or, at the other extreme, a non-locked-in response. These various responses of the near wake give rise to a variety of modifications of the far-wake structure.

A highly coherent, phase-locked flow structure in the far wake is attainable when there is locked-in vortex formation at the carrier frequency f_e in the near wake. This coherent far wake is accomplished by transformation of the flow structure from one dominated by vortex formation at f_e in the near wake, to a structure dominated by the lower sideband component f_m in the far wake. This change in structure corresponds to a large increase in the wavelength and scale of the vortex street relative to the case of purely sinusoidal excitation. The streamwise evolution of the flow structure essentially filters out the spectral components corresponding to the carrier frequency f_e and the upper sideband f_e+f_m.

On the other hand, if the AM excitation induces a non-lock-in response at the carrier frequency f_e, then rapid destabilization of the wake structure can occur. This destabilization, which is characterized by the onset of broadband fluctuations at frequencies below the carrier frequency f_e, is associated with changes in timing of the initially formed vortex relative to the instantaneous displacement of the cylinder from one f_e cycle to the next. As a consequence, the near-wake vortex street, when phase-referenced with respect to the instantaneous cylinder displacement, exhibits large changes at any given streamwise location in the near-wake region. In other words, the AM excitation produces modulations of the phase angle of the initial vortex formation from the cylinder or the arrival of a large-scale vortex at any given streamwise distance, relative to the displacement of the cylinder. Downstream of this near-wake region, the vortical structures interact in such a way that large-scale, incoherent vortical activity dominates the far-wake region. Correspondingly, there is a very large increase in the broadband fluctuation level at low frequencies relative to the case of purely sinusoidal excitation.

The occurrence of the foregoing types of wake response is sensitive to the value of nominal excitation frequency f_e/f_0^*, in particular to whether or not excitation is applied at $f_e/f_0^* = 1.0$. For this case of matched excitation, the flow structure exhibits a locked-in response at the carrier frequency f_e over the entire range of modulation frequency f_m/f_e and dimensionless amplitude Y_e/D considered herein. A slight detuning from this case of matched excitation, to $f_e/f_0^* = 0.95$, allows generation of a rapidly destabilized near wake involving non-lock-in at the carrier frequency f_e. It is important to emphasize that $f_e/f_0^* = 0.95$ corresponds to a locked-in response of the wake structure for the case of purely sinusoidal excitation. We therefore conclude that only a slight detuning from the matched excitation at $f_e/f_0^* = 1.0$ is sufficient to promote rapid destabilization.

The possible states induced by amplitude-modulated excitation can be interpreted as states of increasing disorder in the following sequence: (1) f_m periodic with lock-in at f_e; (2) $2f_m$ periodic with lock-in at f_e over only the second half of the $2f_m$ cycle; and (3) f_m periodic with non-lock-in at f_e occurring for each f_m cycle. We interpret the transformation from state 1 to state 2 as going from a stable response of the near wake to a partially destabilized one. Transformation to state 3 would then represent attainment of a fully destabilized near wake.

Onset of the period-doubled response at $\frac{1}{2}f_m$ would seem to be analogous to the occurrence of the first period doubling observed in the closed system of the Rayleigh–Bénard instability. Although further period doublings corresponding to $4f_m$ and $8f_m$ were sometimes observed, at smaller excitation amplitude the videotape records of the flow visualization were not sufficiently long to allow their characterizations. In general, our impression is that these further period doublings are difficult to achieve and maintain. The occurrence of a well-defined first period doubling, but delicate and somewhat inconsistent further period doubling, has been reported in the Rayleigh–Benard instability studies of Gollub & Benson (1980), as well as in the self-excited system of flow through the end of a cantilever-mounted pipe undergoing elastic oscillations, investigated by Paidoussis & Moon (1988).

The authors gratefully acknowledge support of the Office of Naval Research and the National Science Foundation.

REFERENCES

CHOMAZ, J. M., HUERRE, P. & REDEKOPP, L. T. 1988 Bifurcations to local and global modes in spatially developing flows. *Phys. Rev. Lett.* **60**, 25–28.

CIMBALA, J. M., NAGIB, H. M. & ROSHKO, A. 1988 Large structure in the far wakes of two-dimensional bluff-bodies. *J. Fluid Mech.* **190**, 265–298.

COUDER, Y. & BASDEVANT, C. 1986 Experimental and numerical studies of vortex-couples in two-dimensional flow. *J. Fluid Mech.* **173**, 225–251.

DETEMPLE-LAAKE, E. & ECKELMANN, H. 1989 A phenomenology of Karman vortex streets in oscillating flow. *Expts Fluids* **7**, 217–227.

GOLLUB, J. P. & BENSON, S. V. 1980 Many routes to turbulent convention. *J. Fluid Mech.* **100**, 449–470.

GOODYEAR, C. C. 1971 *Signals and Information.* Wiley Interscience.

GRIFFIN, O. M. & RAMBERG, S. E. 1974 The vortex-street wakes of vibrating cylinders. *J. Fluid Mech.* **66**, 553–576.

GRIFFIN, O. M. & RAMBERG, S. E. 1976 Vortex shedding vibrating in-line with an incident uniform flow. *J. Fluid Mech.* **75**, 257–271.

GRIFFIN, O. M. & VOTAW, C. W. 1972 The vortex street in the wake of a vibrating cylinder. *J. Fluid Mech.* **55**, 31–48.

GURSUL, I., LUSSEYRAN, D. & ROCKWELL, D. 1990 On interpretation of flow visualization of unsteady shear flows. *Expts Fluids* **9**, 257–266.

HUERRE, P. & MONKEWITZ, P. A. 1985 Absolute and convective instabilities in free shear layers. *J. Fluid Mech.* **159**, 151–168.

HUERRE, P. & MONKEWITZ, P. A. 1990 Local and global instabilities in spatially developing flows. *Ann. Rev. Fluid Mech.* **22**, 473–538.

KARNIADAKIS, G. E. & TRIANTAFYLLOU, G. S. 1989*a* Frequency selection and asymptotic states in laminar wakes. *J. Fluid Mech.* **199**, 441–469.

KARNIADAKIS, G. E. & TRIANTAFYLLOU, G. S. 1989*b* The crisis of transport measures in chaotic flow past a cylinder. *Phys. Fluids* A **1**, 628–630.

KOCH, W. 1985 Local instability characteristics and frequency determination of self-excited wake flows. *J. Sound Vib.* **99**, 53–83.

MONKEWITZ, P. A. 1988 The absolute and convective nature of instability in two-dimensional wakes at low Reynolds number. *Phys. Fluids* **31**, 999–1006.

MONKEWITZ, P. A. & NGUYEN, L. N. 1987 Absolute instability in the near-wake of two-dimensional bluff bodies. *J. Fluids Struct.* **1**, 165–184.

NAKANO, M. & ROCKWELL, D. 1991*a* Destabilization of the Karman vortex street by frequency-modulated excitation. *Phys. Fluids* **3**, 723–725.

NAKANO, M. & ROCKWELL, D. 1991*b* Decoupling of locked-in vortex formation by amplitude-modulated excitation. *Phys. Fluids* A **3**, 723–725.

NUZZI, F., MAGNESS, C. & ROCKWELL, D. 1992 Three-dimensional vortex formation from an oscillating, non-uniform cylinder. *J. Fluid Mech.* **238**, 31–54.

OLINGER, D. J. & SREENIVASAN, K. R. 1988 Nonlinear dynamics of the wake of an oscillating cylinder. *Phys. Rev. Lett.* **60**, 797–800.

ONGOREN, A. & ROCKWELL, D. 1988*a* Flow structure from an oscillating cylinder. Part 1. Mechanisms of phase shift and recovery of the near wake. *J. Fluid Mech.* **191**, 197–223.

ONGOREN, A. & ROCKWELL, D. 1988*b* Flow structure from an oscillating cylinder. Part 2. Mode competition in the near wake. *J. Fluid Mech.* **191**, 225–245.

PAIDOUSSIS, M. E. & MOON, F. C. 1988 Nonlinear and chaotic fluidelastic vibrations of a flexible pipe conveying fluid. *J. Fluids Struct.* **2**, 567 591.

ROCKWELL, D. 1990 Active control of globally unstable separated flows. In *Intl Symp. on Nonsteady Fluid Dynamics* (ed. J. A. Miller & D. P. Telionis). FED, vol. 92, pp. 379–394. ASME.

ROCKWELL, D., NUZZI, F. & MAGNESS, C. 1991 Period-doubling in the wake of a three-dimensional cylinder. *Phys. Fluids* A **3**, 1477–1478.

SREENIVASAN, K. R. 1985 Transition and turbulence in fluid flows and low-dimensional chaos. In *Frontiers in Fluid Mechanics* (ed. S. H. Davis & J. L. Lumley), pp. 41–67. Springer.

TRIANTAFYLLOU, G. S. & KARNIADAKIS, G. E. 1989 Forces on a cylinder oscillating in a steady crowflow. In *Proc. Eighth OMAE Conf., The Hague*, Vol. II, pp. 247–252.

TRIANTAFYLLOU, G. S., TRIANTAFYLLOU, M. S. & CHRYSSOSTOMODIS, C. 1986 On the formation of vortex streets behind circular cylinders. *J. Fluid Mech.* **170**, 461–477.

VAN ATTA, C. W. & GHARIB, M. 1987 Ordered and chaotic vortex streets behind circular cylinders at low Reynolds numbers. *J. Fluid Mech.* **171**, 113–133.

WILLIAMSON, C. & ROSHKO, A. 1988 Vortex formation in the wake of an oscillating cylinder. *J. Fluid Struct.* **2**, 355–381.